

SOX10 Single Transcription Factor-Based Fast and Efficient Generation of Oligodendrocytes from Human Pluripotent Stem Cells

Juan Antonio García-León,^{1,*} Manoj Kumar,¹ Ruben Boon,¹ David Chau,² Jennifer One,² Esther Wolfs,³ Kristel Eggermont,¹ Pieter Berckmans,¹ Nilhan Gunhanlar,⁴ Femke de Vrij,⁴ Bas Lendemeijer,⁴ Benjamin Pavie,^{5,7} Nikky Corthout,^{5,7} Steven A. Kushner,⁴ José Carlos Dávila,^{6,8} Ivo Lambrichts,³ Wei-Shou Hu,² and Catherine M. Verfaillie^{1,*}

¹Department of Development and Regeneration, Stem Cell Biology and Embryology, KU Leuven Stem Cell Institute, Herestraat 49, Onderwijs en Navorsing 4, Box 804, 3000 Leuven, Belgium

²Department of Chemical Engineering and Materials Science, University of Minnesota, 421 Washington Avenue Southeast, Minneapolis, MN 55455, USA

³Laboratory of Morphology, Biomedical Research Institute (BIOMED), Hasselt University, Agoralaan, Building C, 3590 Diepenbeek, Belgium

⁴Department of Psychiatry, Erasmus MC, 3015 CE Rotterdam, the Netherlands

⁵VIB Center for Brain and Disease Research, VIB-Leuven, 3000 Leuven, Belgium

⁶Department of Cell Biology, Genetics and Physiology, Faculty of Sciences, Research Biomedical Institute of Málaga (IBIMA), University of Málaga, Campus de Teatinos s/n, 29010 Málaga, Spain

⁷VIB Bio Imaging Core, KU Leuven, Herestraat 49, 3000 Leuven, Belgium

⁸Center for Networked Biomedical Research on Neurodegenerative Diseases (CIBERNED), Madrid, Spain

*Correspondence: jgarleon@hotmail.com (J.A.G.-L.), catherine.verfaillie@kuleuven.be (C.M.V.)

<https://doi.org/10.1016/j.stemcr.2017.12.014>

SUMMARY

Scarce access to primary samples and lack of efficient protocols to generate oligodendrocytes (OLs) from human pluripotent stem cells (hPSCs) are hampering our understanding of OL biology and the development of novel therapies. Here, we demonstrate that overexpression of the transcription factor *SOX10* is sufficient to generate surface antigen O4-positive (O4⁺) and myelin basic protein-positive OLs from hPSCs in only 22 days, including from patients with multiple sclerosis or amyotrophic lateral sclerosis. The *SOX10*-induced O4⁺ population resembles primary human OLs at the transcriptome level and can myelinate neurons *in vivo*. Using *in vitro* OL-neuron co-cultures, myelination of neurons by OLs can also be demonstrated, which can be adapted to a high-throughput screening format to test the response of pro-myelinating drugs. In conclusion, we provide an approach to generate OLs in a very rapid and efficient manner, which can be used for disease modeling, drug discovery efforts, and potentially for therapeutic OL transplantation.

INTRODUCTION

Oligodendrocytes (OLs) are the central nervous system (CNS) glial cells responsible for axonal myelination. However, the complete roles of OLs are still only partially understood and vary depending on the CNS region wherein they reside (Marques et al., 2016). Myelination in the CNS is essential for proper signal conduction along neuronal axons and for maintaining brain homeostasis. Defects in myelin production and/or maintenance are the predominant pathological feature of several diseases, including leukodystrophies and multiple sclerosis (MS) (Franklin et al., 2012). In addition to myelination, OLs have a role in trophic and metabolic support of neurons, fueling oxidative phosphorylation in the mitochondria of axons. This trophic support is disrupted in amyotrophic lateral sclerosis (ALS), and defects in OL function contribute to ALS onset and progression (Lee et al., 2012b).

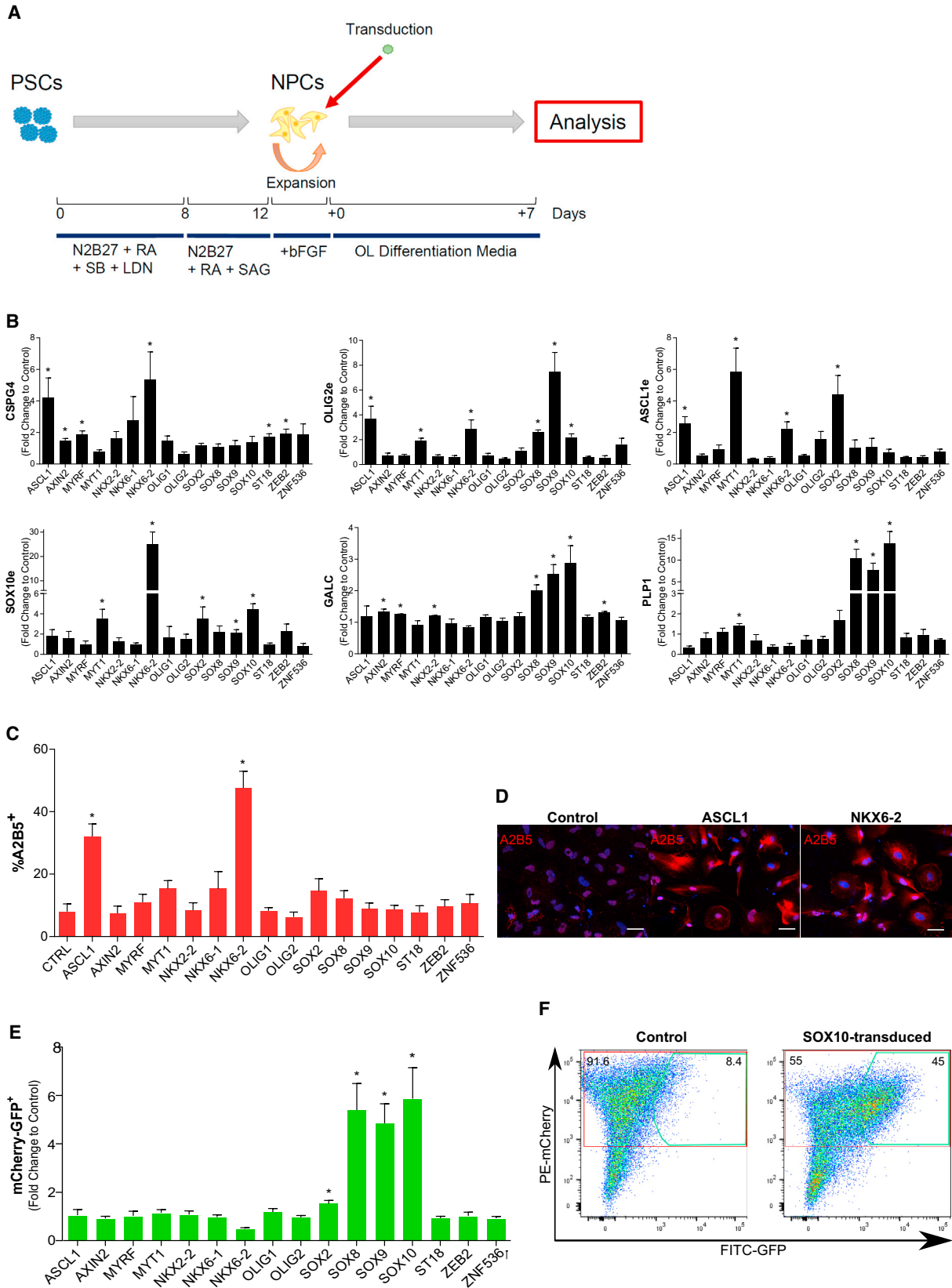
Lack of insight in human OL biology is in large part a consequence of the limited access to human OLs and difficulties in maintaining these cells *in vitro*. Therefore, having access to human OLs would represent a major step forward in studies aimed at understanding mechanisms that are deregulated in diseases with OL involvement. Moreover, this

would allow to test and study if and how candidate drugs affect the process of OL myelination and remyelination (Mei et al., 2014; Lariosa-Willingham et al., 2016), and/or the trophic support provided by OLs.

With the isolation of human embryonic stem cells (hESCs) and the development of human induced pluripotent stem cell (hiPSC) technology, a number of protocols have been developed to generate OLs from hPSCs (Nistor et al., 2005; Hu et al., 2009; Wang et al., 2013; Douvaras et al., 2014), recapitulating *in vitro* the molecular signals and events that occur during *in vivo* OL development, leading to myelinating OLs (Wang et al., 2013; Douvaras et al., 2014). Despite recent optimizations (Douvaras and Fossati, 2015), these protocols remain inefficient and variable in terms of OL yield and, importantly, require very long differentiation times (>100 days to generate myelin basic protein (MBP)-positive OLs). These issues have precluded the use of patient-specific iPSC-derived OLs to elucidate human OL biology and disease, and use such cells as platform for drug screening.

Here, we describe that, by the overexpression of the single transcription factor (TF) *SOX10* in hPSC-derived neural precursors (NPCs), it is possible to generate surface antigen O4 (O4⁺) and MBP⁺ OLs within only ~20 days from





(legend on next page)



the PSC stage. The transcriptome of hPSC-derived O4⁺ cells resembles that of primary intermediate OLs. Similar OL production in terms of efficiency and time course was obtained from patients with MS or familial ALS (fALS) compared with healthy donors. Finally, grafting into homozygous shiverer (Shi^{-/-}) mouse brain slices and co-culture with hPSC-derived neurons confirmed the myelination capability of SOX10-induced OLs in *in vivo* and *in vitro* contexts. All hPSC-derived OL-neuron co-cultures were also adapted to high-throughput screening (HTS) formats allowing demonstration of enhanced myelin production by different compounds.

RESULTS

Selection of TFs Involved in OL Specification

To define which TFs could promote efficient OL differentiation from hPSCs, we selected 16 TFs known to function in OL specification and/or maturation: *ASCL1*, *AXIN2*, *MYRF*, *MYT1*, *OLIG1*, *OLIG2*, *NKX2-2*, *NKX6-1*, *NKX6-2*, *SOX2*, *SOX8*, *SOX9*, *SOX10*, *ST18*, *ZEB2*, and *ZNF536* (Cahoy et al., 2008; Pozniak et al., 2010; Weng et al., 2012; Najm et al., 2013; Yang et al., 2013). The coding regions of these genes were individually cloned in the FUW lentiviral doxycycline-inducible expression vector. As reported (Carey et al., 2009), we demonstrated efficient overexpression of each TF in an inducible manner in our experimental settings (Figures S1A and S1B).

Initial Screening

An initial screen of the 16 selected TFs was performed to identify TFs that induced early, intermediate, and late OL fate. NPCs were generated from hPSCs by dual SMAD inhibition in the presence of retinoic acid (RA) and Sonic hedgehog (SHH) agonist (Chambers et al., 2009). More than 95% of the day 12 PSC progeny stained positive for NPC markers (*SOX2* and *NESTIN*) and most of them (81.8% ± 2.7%) expressed the ventral progenitor marker *HOXB4* (Figure S1C). NPCs were further expanded using basic fibroblast growth factor (bFGF), and then transduced

with each of the 16 individual TFs and cultured in OL differentiation medium (Figure 1A).

To identify the TFs that enhanced OL lineage differentiation, we performed qRT-PCRs for early (*OLIG2* and *CSPG4*), intermediate (*ASCL1* and *SOX10*), and late (*GALC* and *PLP1*) OL lineage markers 7 days after transduction (Figure 1B). Overexpression of *ASCL1*, *NKX6-2*, or *MYT1* induced a significant increase in endogenous (e) transcripts for *OLIG2e*, *CSPG4*, and *ASCL1e*, while expression of the more mature OL genes, *GALC* and *PLP1*, was significantly induced by overexpression of *SOX8*, *SOX9*, or *SOX10*. We also performed immunostaining for A2B5, a marker for intermediate oligodendrocyte precursor cells (OPCs) (Figures 1C and 1D). In the absence of TF overexpression, we detected 8.02% ± 2.46% A2B5⁺ cells, consistent with the fact that differentiation was induced for only 7 days. By contrast, and in line with the qRT-PCR data, 32.05% ± 4.04% and 47.63% ± 5.33% A2B5⁺ cells were identified following overexpression of *ASCL1* and *NKX6-2*, respectively.

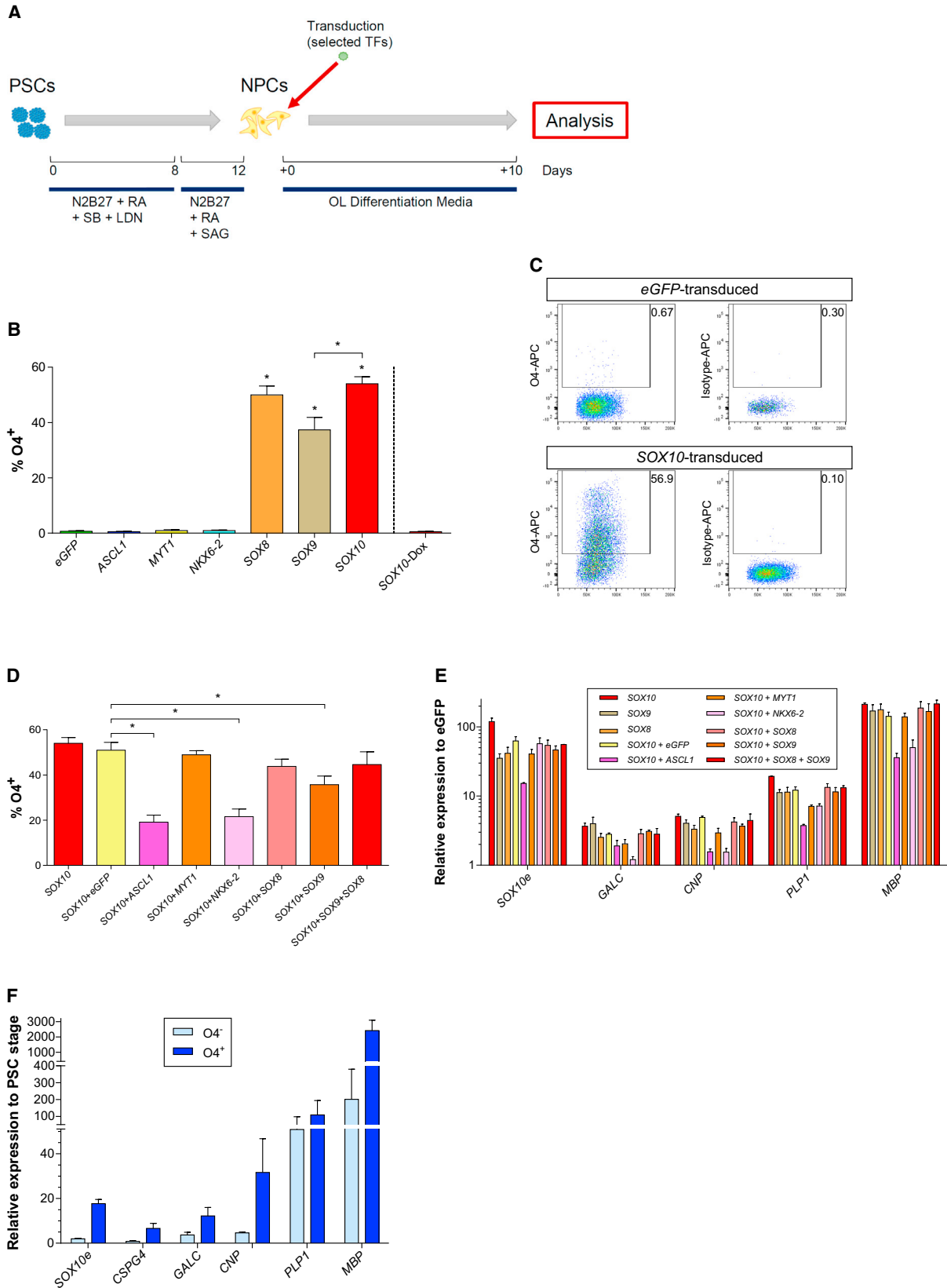
We also transduced the NPCs with a vector containing the MCS5-SOX10 enhancer region, which is an efficient and specific reporter for human OL lineage cells (Pol et al., 2013). Following co-transduction of NPCs with the individual TFs combined with the MCS5-SOX10 vector, expression of GFP (activity of the reporter) was evaluated by fluorescence-activated cell sorting (FACS) 7 days later. As the MCS5-SOX10 vector also contained a constitutive mCherry cassette, the fraction of GFP⁺ cells within the mCherry⁺ population was quantified. A 5- to 6-fold increase in eGFP⁺/mCherry⁺ cells was identified in NPCs transduced with either *SOX8*, *SOX9* or *SOX10*, in line with the increased expression of mature OL markers (Figures 1E and 1F).

Thus, overexpression of *ASCL1*, *NKX6-2*, and *MYT1* induced early-intermediate OL lineage transcripts and proteins, while overexpression of *SOX8*, *SOX9*, and *SOX10* activated the MCS5-SOX10 enhancer-based reporter and induced expression of late OL genes (*GALC* and *PLP1*). The effect of these six TFs was then further analyzed.

Figure 1. Screening of the 16 Selected TFs to Evaluate Their Influence on OL Specification

- Scheme of the strategy followed for NPC generation, expansion and transduction with lentiviral vectors.
- Gene expression changes of early (*CSPG4* and *OLIG2e*), intermediate (*ASCL1e* and *SOX10e*), and late (*GALC* and *PLP1*) OPC markers measured by qRT-PCR, expressed as fold change relative to control (NPCs transduced with *eGFP*).
- Staining for A2B5 in the different transduced cell progeny on day +7.
- Representative images of the A2B5 stainings of vector control and *ASCL1* and *NKX6-2* transduced cells. Hoechst 33258 (blue) was used as nuclear marker.
- Fold change in the expression of the MCS5-SOX10 reporter as a result of the overexpression of the different TFs relative to control (cells transduced with empty vectors) after 7 days in OL differentiation media.
- Example of the expression of the MCS5-SOX10 reporter (GFP-FITC) within mCherry⁺ cells in vector control and *SOX10*-transduced progeny.

Data represented as mean ± SEM of N = 3–4 independent experiments. *p < 0.05. Scale bars: 50 μm.



(legend on next page)



Screening with the Six Selected TFs

We used anti-O4 antibody staining (Sommer and Schachner, 1981) to further define which of the six TFs caused differentiation to mid- and late-stage OL lineage cells. Day 12 NPCs, without bFGF expansion, were transduced with the six TFs individually to enable assessment of the shortest period required to generate OLs from hPSCs, and to avoid possible lineage skewing due to bFGF-based NPC expansion (Furusko et al., 2015). OL differentiation was assessed on day 10 after transduction (22 days from undifferentiated hPSCs) (Figure 2A).

Less than 1% of NPCs transduced with an *eGFP* control vector were O4⁺. Transduction of NPCs with *ASCL1*, *NKX6-2*, or *MYT1* did not increase the fraction of O4⁺ cells, consistent with the finding that these TFs induced immature/intermediate OPC lineage. However, 50.02% ± 3.21%, 37.35% ± 4.51%, and 54.05% ± 2.52% of NPCs transduced with *SOX8*, *SOX9* or *SOX10* were O4⁺, respectively (Figure 2B). We next tested if combined overexpression of *SOX10* with any of the other five TFs would further enhance the proportion of O4⁺ cells. However, no further increase in O4⁺ cells was seen with any TF combination over *SOX10* alone (Figure 2D).

This was confirmed by studies testing OPC/OL marker transcripts in cells transduced with *SOX8*, *SOX9*, or *SOX10* alone, or *SOX10* in combination with the other five TFs (Figure 2E). *SOX10e*, *GALC*, *CNP*, *PLP1*, and *MBP* expression was induced 5- to >100-fold following transduction with *SOX10* alone. Transduction with either *SOX8* or *SOX9* induced similar, albeit somewhat lower levels of these transcripts. Combinations of *SOX10* with any of the other TFs did not further enhance marker expression.

We next FACS sorted O4⁺ and O4⁻ subpopulations 10 days after transduction with *SOX10*. The O4⁺ fraction was highly enriched for cells expressing OPC/OL marker transcripts in comparison with the O4⁻ fraction (Figure 2F), confirming that expression of O4 is specific for intermediate and late OL lineage cells. Thus, overexpression of the TF *SOX10* alone is sufficient to induce differentiation of NPCs toward the OL lineage. Subsequent studies were designed to further characterize the *SOX10*-induced cells.

SOX10-Induced Cells Express Typical Markers of OLs

We next tested if *SOX10*-induced progeny expresses, in addition to O4, other typical OL markers. Immunostaining on day 10 *SOX10*-induced cells (22 days from hPSC stage; without prior O4⁺ enrichment), demonstrated that day 12 NPCs stained positive for OLIG2 but not O4 (Figure 3A), while *SOX10*-transduced cells 10 days after induction were negative for OLIG2 (not shown). Approximately 50%–60% of day 22 NPC progeny stained positive for O4 (in line with the FACS data; Figures 3B, 3C, and 3E) and O1 (Figure S2B), and that 97.15% ± 8.19% *SOX10*⁺ cells co-expressed O4. In addition, 21.48% ± 2.09% *SOX10*⁺ cells also stained positive for MBP (Figures 3D, 3E, and 3G), with 71.67% ± 2.43% of these cells co-expressing MOG (Figure 3H). PLP expression was found as well within the *SOX10*-induced cells (20.35% ± 3.19%), and remained expressed in most (94.60% ± 2.57%) of the O4⁺-purified cells (Figure 3J). These myelin protein-expressing cells displayed a more mature OL morphology, with extended membrane sheaths and highly branched processes (Figures 3C–3J).

Aside from O4⁺ cells, we also found rare TUJ1⁺ neurons (<5%; Figure 3I), but no GFAP⁺ astrocytes in the culture. We also assessed if Schwann cells (SCs) were present in the culture, by staining for the SC-specific peripheral myelin protein 22 (PMP22; Figures S2C and S2D). *SOX10*-induced progeny did not contain PMP22⁺ cells, indicating that only OLs and not peripheral SCs were generated.

To further prove that generation of O4⁺/MBP⁺ cells was due to *SOX10* overexpression, we co-stained *SOX10*-induced progeny with *SOX10* and MBP. All MBP⁺ cells co-expressed *SOX10*, demonstrating that *SOX10* expression was required for the generation of MBP⁺ OLs (Figure 3K). Furthermore, no O4 or MBP expression was observed in *eGFP*-transduced NPCs after 10 days of induction (Figures S2E and S2F).

The yield of O4⁺ cells on day 22 was approximately 240% of the day 12 NPCs, and 24,000% of the day 0 PSCs. This high yield, also from NPCs, reflects the presence of proliferative OPCs in the culture that give rise not only to mature OLs but also to other OPCs. In fact, Ki67⁺ cells were present throughout differentiation (Figure 3L), with 24.22% ± 1.20% of Ki67⁺ cells present in the whole culture on day 10 after *SOX10* induction. However,

Figure 2. Impact of the Six Selected TFs on OPC/OL Specification Alone or in Combination

- Scheme of the strategy followed for NPC generation and direct transduction for a total period of 22 days from the PSC stage.
- Evaluation of the expression of O4 by FACS in NPCs transduced with the selected six TFs alone after 10 days in OL differentiation media.
- Representative dot plots of O4 expression and isotype control by FACS of cells transduced with either *SOX10* or *eGFP*.
- Percentages of O4 expression when NPCs were transduced for 10 days with different combinations of the TFs.
- Gene expression levels of OPC/OL markers 10 days following transduction with single or combinations of the six TFs selected.
- Gene expression levels for OPC/OL markers in FACS sorted O4⁺ and O4⁻ cells 10 days after *SOX10* induction. Expression levels normalized to *GAPDH*. *SOX10e* refers to its endogenous expression.

Data represented as mean ± SEM of N = 3–5 independent experiments. *p < 0.05.

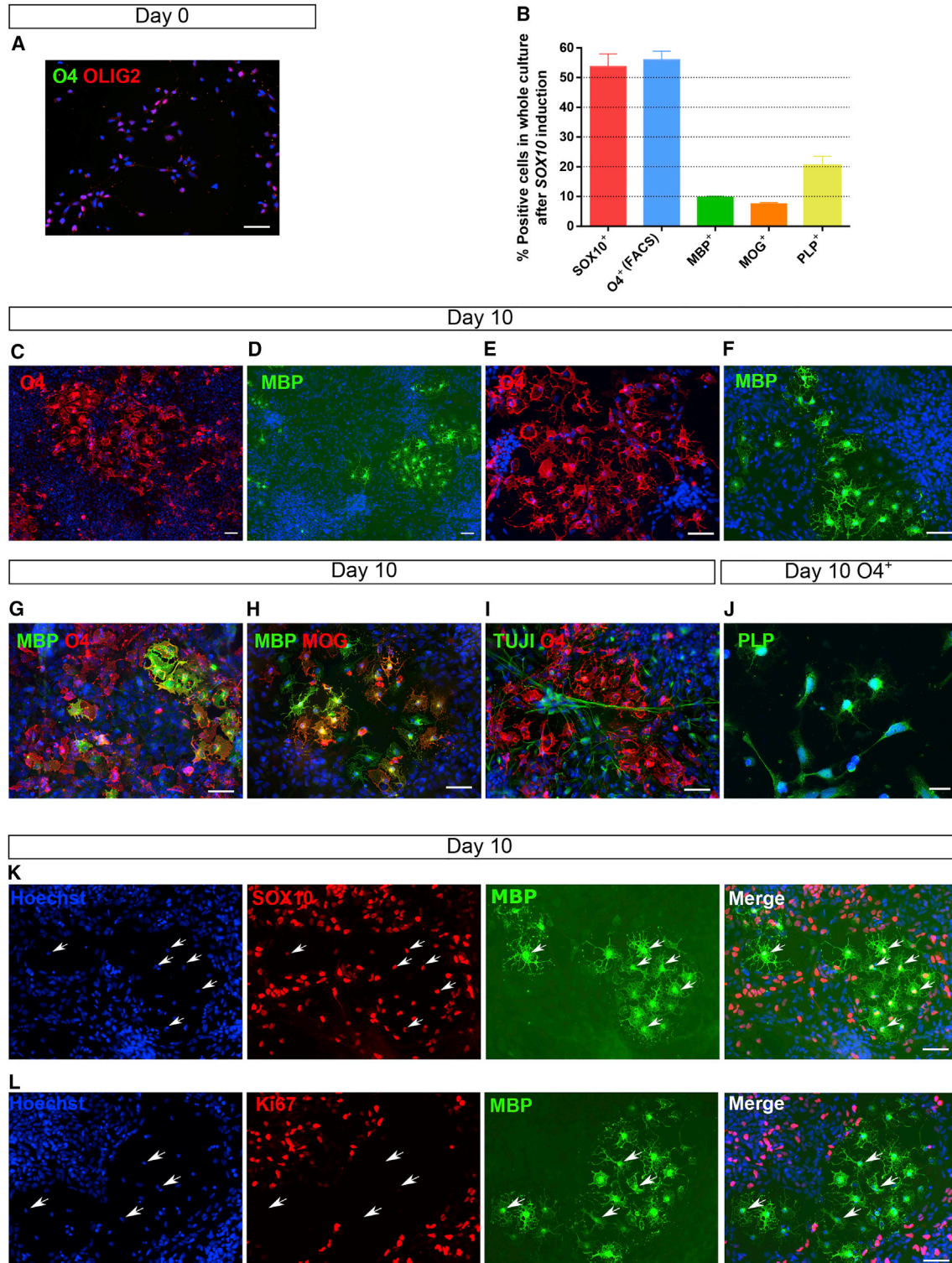


Figure 3. Phenotypic Characterization of SOX10-Induced OLs by Immunocytochemistry

(A) Untransduced NPCs express the early OPC marker OLIG2 but not O4.

(B) Quantification of OPC/OL marker expression in the whole culture after 10 days of SOX10 induction.

(legend continued on next page)



all MBP⁺ cells were Ki67⁻ (Figure 3L), and hence post-mitotic, consistent with the acquisition of a mature OL phenotype.

SOX10-Induced Cells Resemble Primary OLs at the Transcriptome Level

To assess if *SOX10*-induced OLs resembled primary OLs, we performed RNA-sequencing (RNA-seq) on purified O4⁺ cells derived from four different hPSC lines: the hESC H9 and the hiPSC ChiPSC6b, Sigma-iPSC0028, and BJ1 (healthy donor-derived) lines. The transcriptome of the O4⁺ cells was combined with published transcriptome data from different brain cells (GalC⁺ OLs, CD90⁺ neurons, CD45⁺ myeloid cells, HepaCAM⁺ astrocytes, BSL-1⁺ endothelial cells, and the whole cortex) (Zhang et al., 2016; Abiraman et al., 2015).

Principal-component analysis and unsupervised hierarchical clustering on the entire transcriptome identified a very distinct cluster encompassing different brain-derived OL samples, as well as the *SOX10*-induced O4⁺ cells, separated from neurons, astrocytes and other non-ectodermal-derived cells (Figures 4A and 4B). To further characterize the maturity of the generated O4⁺ OLs, we also included samples consisting of immature, intermediate, and mature OLs isolated from human fetal tissues (Abiraman et al., 2015). Comparison of OL-specific markers (Cahoy et al., 2008; Nielsen et al., 2006) revealed that O4⁺ cells derived from H9 and Sigma-iPSC0028 lines co-clustered with intermediate OLs, while ChiPSC6b and BJ1 O4⁺ cells clustered more closely to immature OLs (Figure 4C).

Next, we compared *SOX10*-PSC O4⁺ cells (average values of all PSC-derived cells) with different primary OLs using a sequence alignment map (Figures 4D and 4E). We identified 916 (13.48%) differentially expressed genes between mature OLs and PSC-O4⁺ cells (fold change >2 and false discovery rate < 0.05) (699 up- and 217 downregulated genes in PSC-O4⁺ cells) and 240 (3.53%) differentially expressed genes between intermediate OLs and PSC-O4⁺ cells (all up-regulated in PSC-O4⁺ cells) (Table S1), confirming that O4⁺ cells were highly similar to mature/intermediate primary OLs (Figure 4E). Over 85% (47/53) of OL-specific genes (including *MAG*, *MOG*, *SOX10*, and *OLIG2*) were expressed at comparable levels in O4⁺ cells and primary OLs (Figure 4D).

Lastly, we performed gene ontology (GO) analysis to identify classes of genes that were similarly expressed between O4⁺ hPSC-derived cells and primary OLs. When compared with primary intermediate OLs, a higher number of shared GO pathways were obtained, including those referred to CNS development as well as to OL development (Table S2). In addition, other terms were related to cytoskeleton organization and protein modifications, pathways associated to OLs (Nielsen et al., 2006). Overall, these results support the notion that *SOX10*-induced O4⁺ cells are highly comparable at the transcriptome level with primary OLs, especially intermediate OLs.

Inducible Single-Copy SOX10 Overexpression from the AAVS1 Locus Efficiently Induced OL Cell Conversion

To avoid effects of random integration of the *SOX10* transgene resulting from lentiviral transduction, and also to avoid the use of this technology for OL generation, we created an hESC line wherein *SOX10* was introduced in the safe harbor locus *AAVS1*, using recombinase-mediated cassette exchange in hPSC lines containing an FRT-flanked cassette, which contained a hygromycin-resistance/thymidine kinase selection cassette (Ordovás et al., 2015). This created 100% homogeneous hESCs containing either an *SOX10* or an *SOX10-eGFP* cassette under a doxycycline-inducible promoter (Figures S4A and S4B).

Addition of doxycycline to hESCs induced the expression of *SOX10* or *SOX10-eGFP* in >99% of cells (Figures S4C and S4D). Induction of *SOX10* on day 0, without prior neural commitment, did not result in the generation of MBP⁺ OLs (not shown). When hPSCs were first fated to NPCs for 8 days, followed by addition of doxycycline and culture in OL differentiation medium, already 50% O4⁺ cells were found on day 4, and 89.3% ± 0.6% by day 7, which was sustained at later time points (Figure S4E). The emergence of O4⁺ cells was accompanied by progressively increased levels of OPC/OL markers, in both *SOX10* and *SOX10-eGFP* transgenic lines (Figure S4F). Immunostaining further demonstrated the OL identity of the cells: MBP⁺ cells could be detected by day 7, and its expression increased progressively by day 10 of induction (day 18 of the overall differentiation culture; Figure S4G). No contamination with neurons was observed.

(C–H) Representative images of the cultures showing expression of the OL markers O4, MBP, and MOG. (I) TUJ1⁺ neurons are present in a small proportion.

(J) Expression of the proteolipid protein (PLP) in O4⁺ cells isolated on day 10 following *SOX10* induction.

(K) The expression of *SOX10* was found in all MBP⁺ OLs (exemplified with white arrows).

(L) None of the MBP⁺ OLs expressed the Ki67 marker (exemplified with white arrows), and hence present a postmitotic phenotype.

Representative images of N = 3–5 independent differentiations. Hoechst 33258 (blue) was used as nuclear marker. Scale bars: 50 μm; 20 μm for (J).

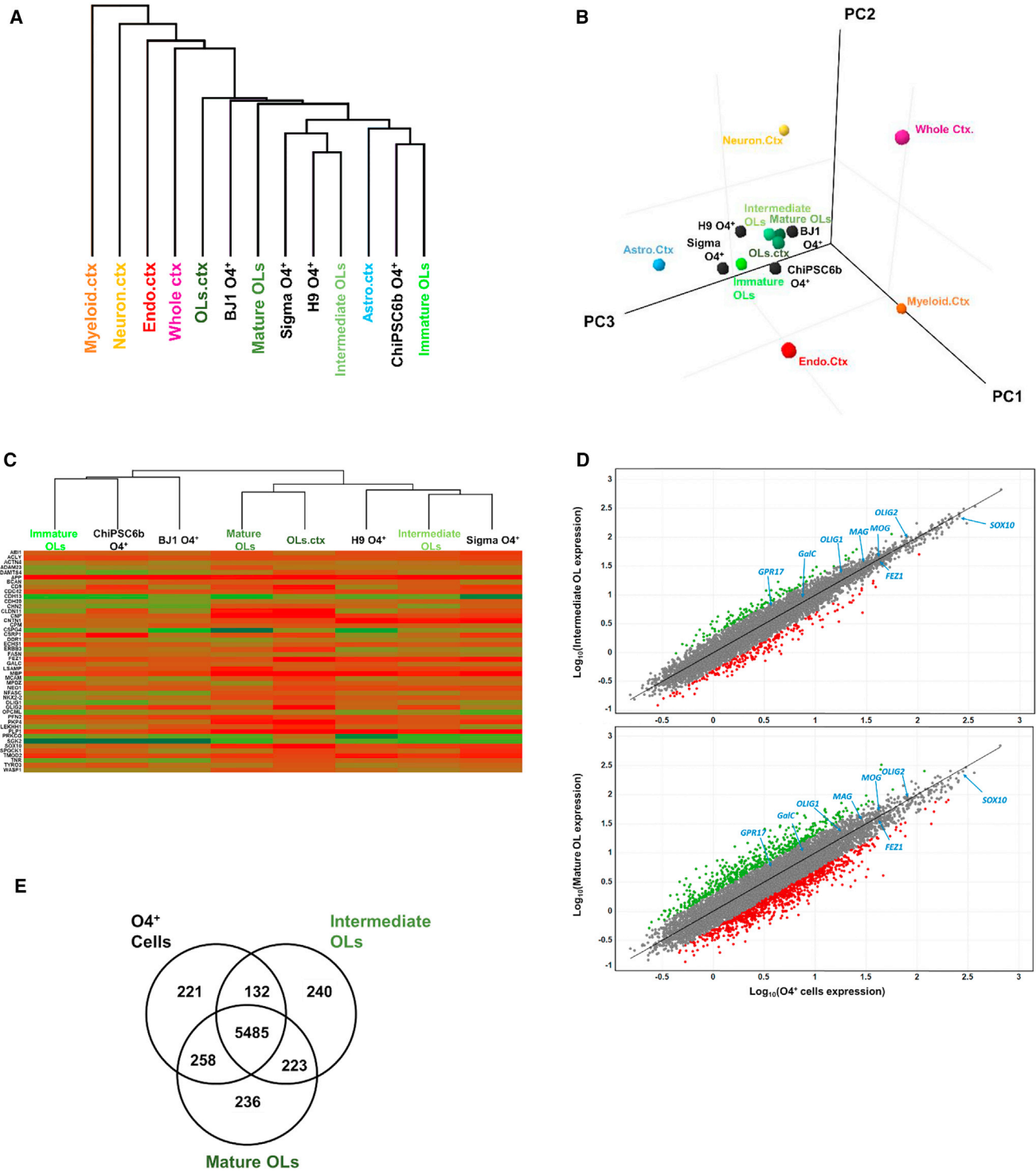


Figure 4. Global Transcriptome Comparison of *SOX10*-Induced Cells with Primary Different Brain Lineages

(A) Hierarchical clustering of whole-genome expression profile of *SOX10*-induced O4⁺ cells (black), different primary OL samples (green), myeloid cells (orange), neurons (yellow), endothelial cells from cortex (red), astrocytes (light blue), and whole cortex (pink).

(B) Principal-component analysis (PCA) of different samples mentioned in (A).

(C) Hierarchical clustering and heatmap comparison of OL-specific markers among PSC-derived O4⁺ cells and primary OLs.

(legend continued on next page)



SOX10-Induced OLs Myelinate Both Shiverer Mouse and hPSC-Derived Cortical Neurons

To demonstrate that *SOX10*-induced O4⁺ cells have functional characteristics of OLs, we tested if they were capable of myelinating neuronal axons. To address myelination in an *in vivo* context, purified O4⁺ cells were injected in brain slices from homozygous shiverer (shi/shi) mice (MBP deficient) and slices were analyzed 10 days later. Immunostaining demonstrated efficient engraftment and homogeneous spreading of the transplanted human hNA⁺ cells within the tissue, with 48.13% ± 4.15% of cells also expressing MBP (Figures 5A–5C). Moreover, MBP⁺ OL projections wrapping NF200⁺ neuronal axons could be observed 10 days after injection (Figures 5D and 5E).

We also assessed if myelination occurred in *in vitro* co-cultures. We generated cortical neurons from human iPSCs as described previously (Shi et al., 2012). Neuronal progenitors were replated and allowed to mature for 10–14 days. O4⁺ cells, isolated and purified on day 10 following *SOX10* induction, were co-cultured with cortical neuronal progeny for an additional 20 days in OL myelination medium. Regions wherein TUJ1⁺ axons were aligned with MBP⁺ OLs could already be seen a few days later (not shown). By day 20 of co-culture, O4⁺ cells extended MBP⁺ regions aligned with axons at multiple locations (Figures 5F–5K). Transverse sections of reconstructed confocal microscopy images demonstrated the presence of MBP⁺ extensions fully wrapping neuronal axons (Figures 5H and 5I). 3D reconstructions also demonstrated the presence of MBP⁺ sheaths surrounding TUJ1⁺ axonal prolongations (Figures 5J and 5K). At the ultrastructural level, cytoplasmic regions of OLs were frequently observed surrounding neuronal axons (Figures 5L and 5M) and were able to form multilayer compact myelin sheaths (Figure 5Q). Early myelination of neuronal axons was also observed (Figures 5O and 5P). These results indicate that *SOX10*-induced OLs matured into myelinating OLs that ensheathed and wrapped axons in both an *in vivo* context, as well as when co-cultured with hPSC-derived neurons *in vitro*.

Efficient Generation of OLs from iPSCs Derived from Patients with MS and ALS

To determine the robustness of the protocol, and to demonstrate that OLs can also be generated from iPSCs of patients with neurodegenerative diseases wherein OLs have been shown to play a causal role, we compared the generation of OLs from hPSCs from healthy donors

(hESC-H9 and hiPSC ChiPSC6b, Sigma-iPSC0028, and BJ1 lines), with iPSC lines from two primary progressive MS (PPMS) patients and from two patients with a familial form of ALS (fALS) caused by mutations in the genes superoxide dismutase (*SOD1A4V*) or *C9ORF72*.

We found no substantial differences in the expression of intermediate and late OL marker transcripts among the eight cell lines analyzed at different time points (Figure 6A). In addition, no significant differences in the efficiency of generating O4⁺ cells were seen among the lines (50%–65% O4⁺ cells; Figure 6B). Finally, approximately 10% of MBP⁺ cells were present on day 22 in the *SOX10*-induced NPC progeny from all lines examined, with the exception of BJ1-derived cells, which contained only 6.34% ± 0.70% MBP⁺ cells (Figure 6C). In addition, MBP⁺ progeny from PSCs of healthy donors and from PPMS and fALS patients had similar morphology (Figure 6D).

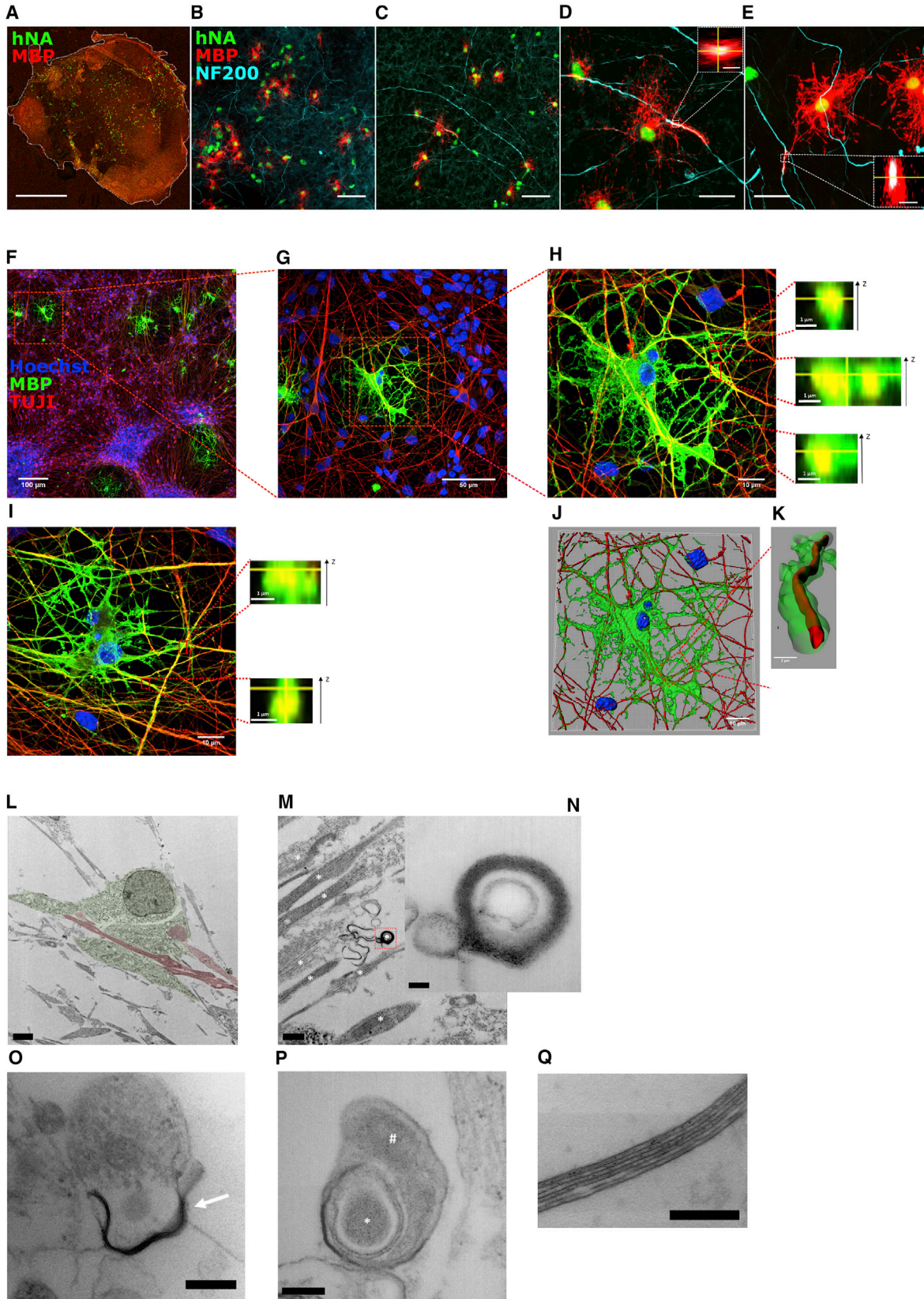
Thus, the *SOX10*-mediated differentiation protocol could generate intermediate and mature OLs with similar efficiencies also from PPMS and fALS iPSC lines only after 22 days of differentiation. This proves the robustness of the protocol irrespective of the iPSC lines used to generate O4⁺/MBP⁺ OLs.

Creation of a Myelinating Co-culture System for High-Throughput Drug Screening

Currently, no good assays are available to identify and validate drugs that can enhance myelination. The existing platforms are based mostly on primary murine OLs cultured in the absence (Mei et al., 2014; Lee et al., 2012a) or presence of neurons (Deshmukh et al., 2013; Lariosa-Willingham et al., 2016). Recently, *in vitro* myelination systems based on murine PSCs suitable for high-throughput screening (HTS) have been developed (Najm et al., 2015; Kerman et al., 2015). However, such a model using hPSC-derived neuronal and OL progeny has not yet been described.

To enable HTS approaches, we adapted and optimized the cortical neuron-OL co-culture system to 96- and 384-well plate format. Following induction of *SOX10* for 10 days, purified O4⁺ cells could be cryopreserved, with >90% cells remaining viable and functional after thawing (not shown). To test if hPSC-derived neuron-OL co-cultures allow identification of myelination-enhancing factors (e.g., triiodothyronine, T3) or different medications, *SOX10*-induced purified O4⁺ cells were cultured on top of maturing neurons for 20 days, and expression of MBP

(D) Pairwise scatterplot of log₁₀ gene expression of PSC-derived O4⁺ cells (N = 12) versus intermediate (N = 6) and mature (N = 3) primary OLs. Gray, genes expressed at similar levels (<2-fold difference), with blue arrows identifying key OL-specific genes; red and green dots, genes that are >2-fold higher or >2-fold less expressed in PSC-derived O4⁺ cells compared with primary intermediate and mature OLs. (E) Venn diagram depicting the number of genes expressed in common or differently (>2-fold change) in *SOX10*-induced O4⁺ cells and primary intermediate and mature OLs.



(legend on next page)



evaluated. Co-cultures were supplemented or not with two drugs identified in a murine stem cell-derived HTS to enhance MBP⁺ expression, miconazole and clobetasol (Najm et al., 2015). In addition, we tested the effect of the γ -secretase and Notch signaling inhibitor DAPT, reported to have a positive influence on *in vitro* myelination of murine OPCs (Lariosa-Willingham et al., 2016), and pranlukast, a blocker of the olig2-targeted G-protein-coupled receptor Gpr17, reported to enhance remyelination and OL survival, but not yet tested in *in vitro* screens (Ou et al., 2016). The readout included assessment of the total MBP⁺ area, number of MBP⁺ cells, and MBP⁺ intensity (Figure 7).

MBP expression increased 1.5- to 2-fold when T3 was added compared with control (DMSO) conditions (Marta et al., 1998). Miconazole induced a similar increase, and addition of pranlukast induced a 1.5- to 2.5-fold increase in MBP expression. The highest levels of MBP expression were observed for clobetasol, reaching a 3- to 4-fold increase of MBP expression compared with control, which was significantly higher than the effect of T3 when matched-pair analysis was performed (Figure S5). By contrast, DAPT did not enhance MBP expression. Similar results were obtained in both 96- and 384-well assay formats (Figure 7A), with little variation between intra- or inter-plate replicates, and for all three MBP-staining readouts.

Thus, the fully human neuron-OL co-culture system described here can be successfully scaled across multiple formats, allowing HTS to identify and validate compounds involved in myelination. This system could be used as well to study the mechanisms underlying OL-mediated neuronal dysfunction or death.

DISCUSSION

Our understanding of the complex OL biology and mechanisms underlying several OL diseases has been limited

by the difficulties of obtaining human OLs. Since the implementation of hESCs/hiPSC technology, different methods have been described whereby OLs can be generated from hPSCs (Nistor et al., 2005; Hu et al., 2009; Wang et al., 2013; Douvaras et al., 2014), but inefficiently and, therefore, impeding the use of these cells for disease modeling or drug development.

To overcome these issues, we hypothesized that overexpression of TFs known to play a role in OL specification and/or maturation would enhance the efficiency as well as the speed with which OL could be generated from hPSCs. We selected 16 TFs known to regulate human and/or murine OL specification and/or maturation (Cahoy et al., 2008; Pozniak et al., 2010; Weng et al., 2012; Najm et al., 2013; Yang et al., 2013) and tested if their overexpression would enhance OPC/OL fating. By a combination of methods, we demonstrated that overexpression of *SOX10* alone in NPCs induced ~60% of cells expressing O4, of which 20% also co-expressed the myelin protein MBP.

The *SOX* genes are TFs with a characteristic high-mobility group domain, involved in developmental specification and classified into nine groups based on sequence similarity and function (Wegner, 2010). Among them, the *SOXE* group of TFs, composed of *SOX8*, *SOX9* and *SOX10*, is involved in specification of myelinating glial cells, both SCs and OLs (Weider and Wegner, 2017). We obtained late OPC specification when either *SOX8*, *SOX9* or *SOX10* were overexpressed, consistent with the previously described role of these TFs during OL specification. Although redundant functions have been described for these three TFs due to the high sequence preservation of the functional domains, *Sox10* is considered as the main *Sox* TF regulating OL specification and maturation, with also epigenetic functions (Weider et al., 2013; Vogl et al., 2013). As *SOX10* is known to be involved in SC development (Weider et al., 2013), we also assessed if SCs were concomitantly induced in our cultures. However, we could

Figure 5. *SOX10*-Induced OLs Myelinate Both Shiverer Mouse Brain Slices and hPSC-Derived Cortical Neurons

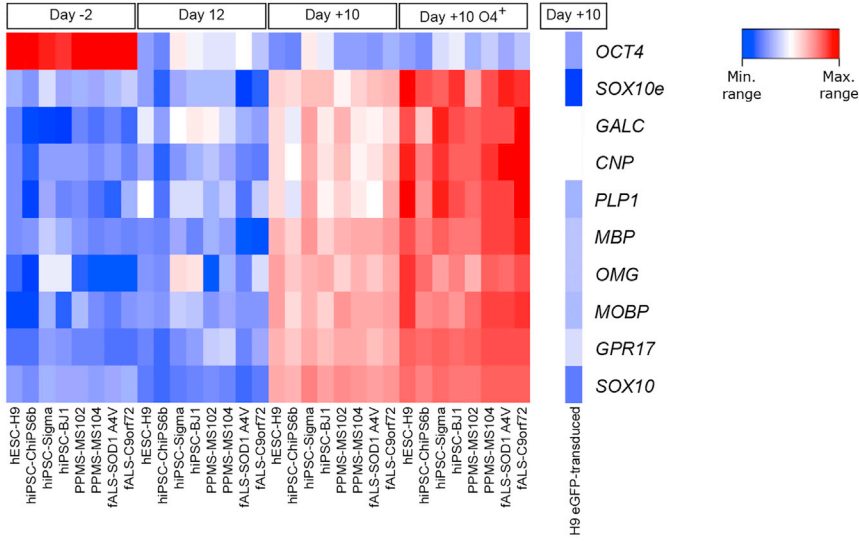
(A–E) Confocal microscopy images of O4⁺ purified *SOX10*-induced cells injected into *Shi*^{-/-} mouse brain slices 10 days after injection. (A) Whole-slice image showing homogeneous dispersion of the injected cells (human nuclear antigen, hNA⁺). (B and C) Overview images of slices showing grafting and maturation of the injected cells. (D and E) Detailed images showing MBP⁺ prolongations annealing and ensheathing NF200⁺ neuronal axons.

(F–Q) Confocal and transmission electron microscopy (TEM) images of the co-culture between hPSC-derived neurons and *SOX10*-induced O4⁺ cells. (F) Overview of the co-culture. (G) Amplification of a representative region with mature OLs extending their processes over neuronal axons. (H and I) Magnifications of an OL showing, at different locations, the complete ensheathment of neuronal axons. (J) 3D reconstruction suggesting the wrapping of axons by an OL. (K) Detailed 3D reconstruction of a region showing complete ensheathment of an axon (red) by MBP⁺ prolongations (green). Nuclei counterstained with Hoechst 33258 (blue). (L) TEM image showing neuronal axons (red) surrounded by an OL (green). (M) Myelin-like structures are found in regions with axon tracts. (N) Magnification of a myelinating structure where compact myelin formation can be observed. (O) TEM example where myelination of a neuronal axon is partially complete (arrow). (P) Detailed micrograph of an OL prolongation (#) starting to form a layered myelin sheet around a neuronal structure (*). (Q) Magnification showing the formation of a multilayer compact myelin structure.

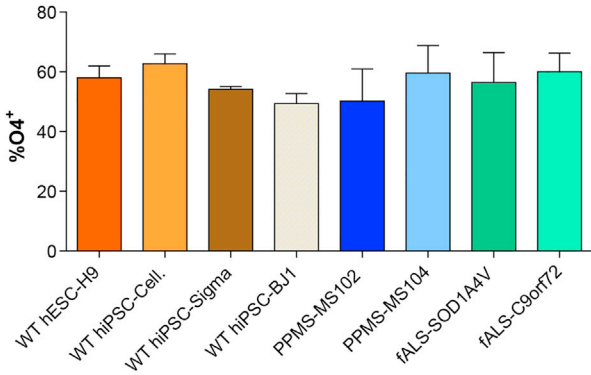
Scale bars: 1 mm (A), 50 μ m (B and C), 20 and 2 μ m inserts (D and E), 2 μ m (L), 0.5 μ m (M), 100 nm (N), 200 nm (O), 200 nm (P), and 200 nm (Q).



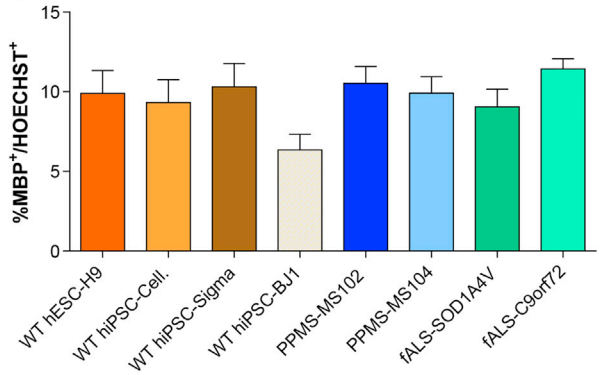
A



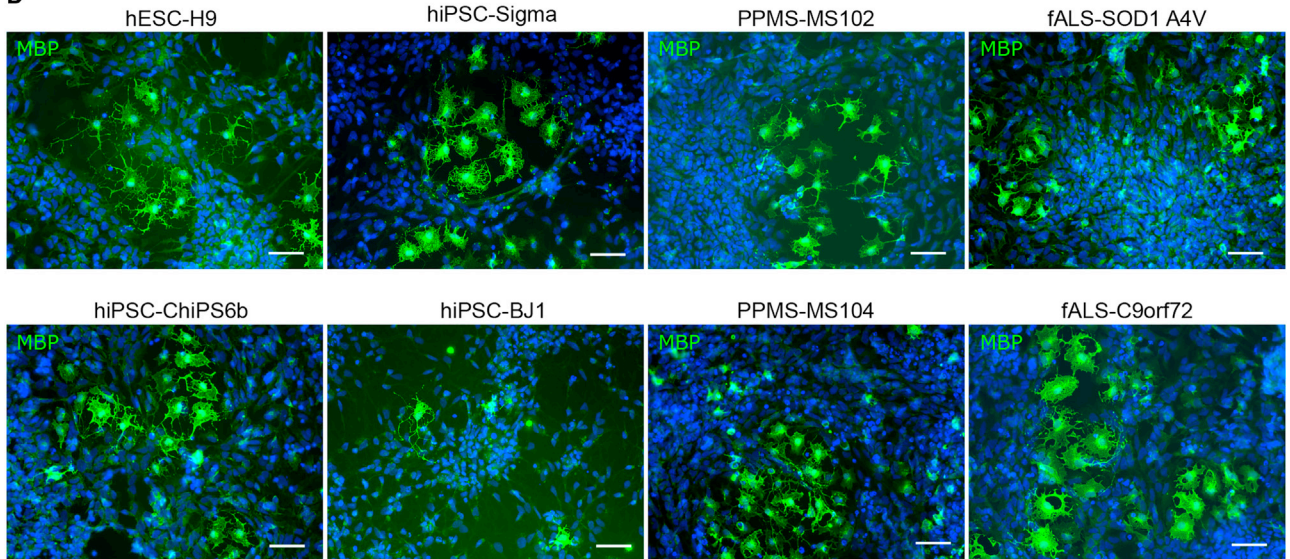
B



C



D



(legend on next page)



not detect cells with typical SC markers. Thus, although *SOX10* plays a role in maturation and myelin production of both cell types, the lack of SC induction in our assay is likely due to the fact that the NPC and subsequent differentiation conditions are OL specific and not supportive for SC development, in line with their differential developmental origin compared with OLs (Zawadzka et al., 2010).

The basic helix-loop-helix protein OL lineage transcription factor 2 (*Olig2*) is considered to be the main TF responsible for OPC specification. Most OPCs generated from NPCs in the motor neuron progenitor region of the spinal cord express *Olig2*, and *Olig2* is believed to orchestrate OL differentiation by inducing the expression of *Nkx2.2* and later that of *Sox10* (Sim et al., 2011). To mimic conditions present in the motor neuron progenitor region during NPC induction from PSCs, we combined dual SMAD inhibition with the caudalizing and ventralizing factors, RA and SHH agonist, respectively. This resulted in $51.7\% \pm 4.6\%$ of NPCs that expressed OLIG2 and $81.76\% \pm 2.67\%$ the ventral marker HOXB4 (Franklin et al., 2012; Lee et al., 2012b). Overexpression of *SOX10* alone in these NPCs resulted in the specification and maturation of OLs. However, overexpression of *SOX10* in uncommitted hPSCs did not result in OPCs and differentiation (not shown), demonstrating that *SOX10* alone cannot directly induce an OL fate in hPSCs, but only in already neural-committed precursors. Of note, we did not detect neural/glial antigen 2 (NG2)- or platelet-derived growth factor receptor α (PDGFR α)-positive cells following *SOX10* overexpression, suggesting that *SOX10* causes the direct generation of late OPCs/OLs from *OLIG2*⁺ NPCs without an intermediate OPC stage.

Recently, Ehrlich et al. (2017) published a protocol for OL generation from hPSCs also based on TF overexpression. They demonstrated that *SOX10* was the only TF capable of inducing O4 expression, which was further enhanced when combined with *OLIG2* and *NKX6.2*. They observed a similar frequency of O4⁺ cells and final maturation to MBP⁺ OLs at the end of differentiation as we describe here. However, the Ehrlich et al. protocol required 28 days to generate ~70% O4⁺ cells, and an additional 7 days for efficient MBP⁺ OL production after NPC

transduction. By contrast, our protocol requires 10 days following NPC transduction with *SOX10* to generate similar levels of O4⁺ cells of which 20% also express MBP.

Although the reasons for the different requirement of three versus one TF to generate O4⁺ cells from NPC are not clear, we hypothesize that these differences might be due to differences in the initial NPC generation. Ehrlich et al. induced neural specification via embryoid bodies in the presence of SMAD inhibitors and the Wnt activator and caudalizing molecule CHIR99021, combined with the ventralizing SHH agonist Purmorphamine. By contrast, we induced NPCs by dual SMAD inhibition in adherent cultures, and in the presence of low concentrations of RA, essential for efficient generation of *OLIG2*⁺ precursors and subsequent OPC specification (Douvras et al., 2014). The fact that we only need the single TF *SOX10* may allow future studies to develop methods that will directly or indirectly target endogenous *SOX10* to generate OLs that could be used clinically.

To further characterize the OL progeny, we performed RNA-seq analysis on day 22 O4⁺-purified OLs, and compared their transcriptome with previously described datasets from primary neural populations including immature to mature OLs (Zhang et al., 2014, 2016; Abiraman et al., 2015). This demonstrated that *SOX10*-induced O4⁺-purified cells clustered with *bona fide* OLs and differed from other brain cells. We found slight discrepancies in the levels of OL maturity among the four lines tested, which may be the consequence of variability between cells from which O4⁺ cells were derived, as these cells have different developmental origins, are derived from genetically distinct individuals and/or hiPSCs may differ in their level of epigenetic reprogramming (Bilic and Izpisua Belmonte, 2012). In addition, we included in the analysis the OLs described by Ehrlich et al. (2017) (Figure S3), finding that all OLs clustered together and the OLs generated by both studies presented highly shared transcriptomes with primary OLs, indicating that TF-induced OLs resemble primary OLs at the transcriptome level.

The robustness of the protocol was further validated by deriving OLs from two MS and two fALS patients. These MS/fALS patient-derived OLs expressed similar markers

Figure 6. Generation of OLs from Different Lines Including MS and fALS Patients

(A) Heatmaps of qRT-PCR analysis performed at different stages of OPC/OL differentiation induced by *SOX10* overexpression comparing the eight different hPSCs used: four lines derived from healthy donors (hESC-H9, hiPSCs ChiPSC6b, Sigma, and BJ1), two from primary progressive MS patients (PPMS-102 and -104), and two from patients with familial ALS with mutations in SOD1 (fALS-SOD1 A4V) and C9orf72 (fALS-C9orf72) (*SOX10e* = endogenous *SOX10*).

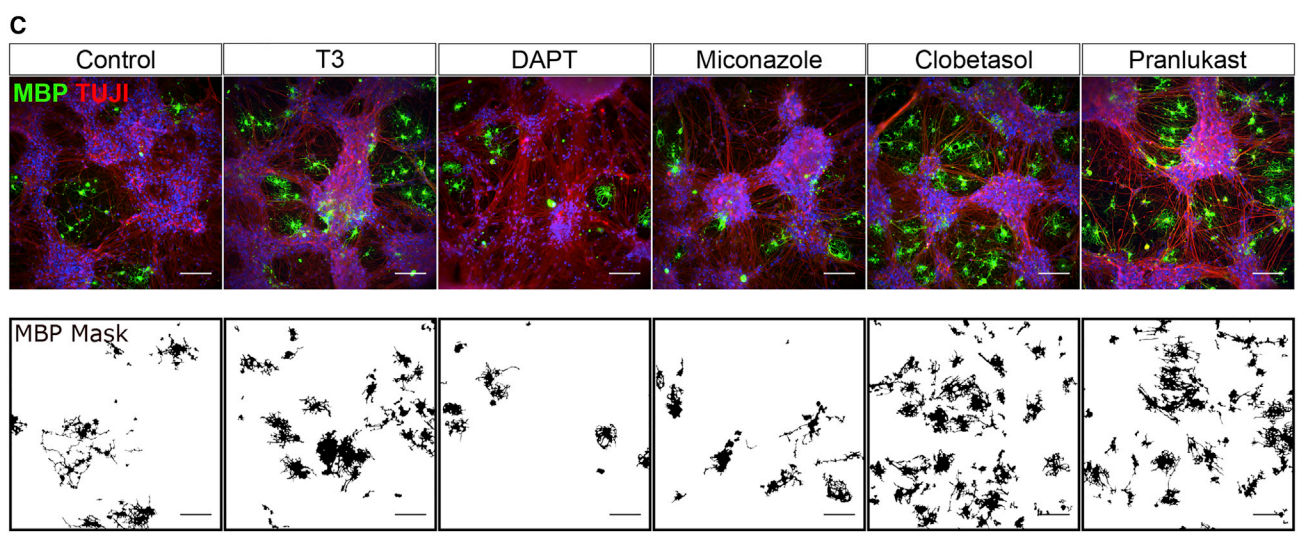
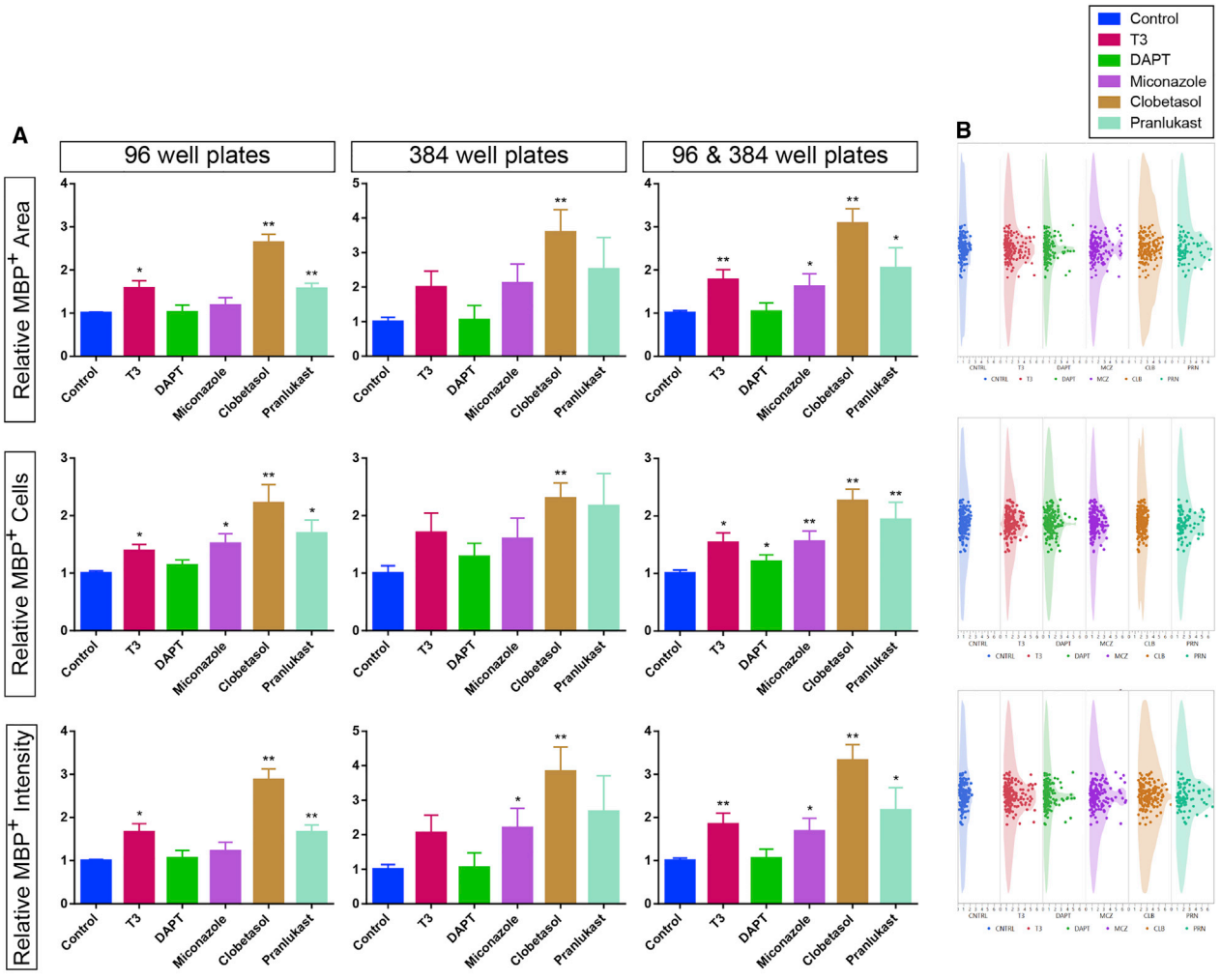
(B) O4 expression by FACS of the eight hPSC lines analyzed after 10 days in OL differentiation medium.

(C) Quantification of the total percentage of MBP⁺ cells.

(D) Representative images of MBP⁺ OLs obtained after 10 days from the eight hPSC lines.

Hoechst 33258 (blue) was used as nuclear marker. Scale bars: 50 μ m.

Data represented as mean \pm SEM of N = 3 independent experiments per line.



(legend on next page)



and morphology compared with healthy donor-derived cells. Among the eight lines tested, the only significant difference we found was a reduction in the proportion of MBP⁺ cells in *SOX10*-induced cells from the BJ1 line (Figure 6C). Notably, we also found a reduction in the percentage of the OLIG2⁺ population (51.7% versus 30.7%) after 12 days of neural induction in BJ1 cells. As hiPSCs may have skewed capacities to the differentiation toward different lineages (Bilic and Izpisua Belmonte, 2012), we hypothesize that decreased neural differentiation capacity of the BJ1 iPSCs may determine the lower frequency of mature OLs obtained at the end of the *SOX10*-induced protocol.

To evaluate the myelination capacity of *SOX10*-induced O4⁺ OLs, we first injected the cells into MBP^{-/-} homozygous shiverer mouse brain slices and demonstrated not only efficient engraftment and dispersion within the slice, but also wrapping of neuronal axons by MBP⁺ OL prolongations in this *in vivo* context 10 days after injection. To further demonstrate the myelinating capabilities of generated O4⁺ cells *in vitro*, we established a fully hPSC-derived co-culture system, demonstrating that induced OLs were able to produce MBP⁺ extensions aligning with neuronal axons and myelin ensheathment by about 20 days following co-culture, even though *SOX10* was no longer overexpressed during the last 10 days of the co-culture, suggesting that *SOX10* overexpression was no longer required at this stage to support OL maturation and myelination. Myelin formation surrounding axons and the presence of compact multi-layered myelin was also observed in the co-culture system at the ultrastructural level, fully demonstrating the myelination capacity of *SOX10*-derived OLs.

To enable HTS for drugs that improve myelination, we successfully adapted the co-culture system to 96- and 384-well plate formats. This allowed us to demonstrate that MBP expression increased considerably when T3, a known inducer of myelin production (Marta et al., 1998), was added to the medium. Clobetasol, previously shown to enhance myelination both *in vitro* and *in vivo* (Najm et al., 2015), increased MBP expression to even higher

levels than T3. MBP expression was also induced by miconazole, but to a lesser extent. Increase in MBP staining was also seen after treatment with pranlukast, a compound known to inhibit signaling via the Gpr17 receptor, and reported to enhance remyelination and OL survival in mouse (Ou et al., 2016). As this occurred already at the μ M level, pranlukast might be an interesting drug candidate to be tested for (re)myelination in pathological conditions (Mogha et al., 2016). However, DAPT did not significantly increase MBP staining, in contrast with previous studies (Lariosa-Willingham et al., 2016). Differences in myelin production might be due to the fact that we tested the effect of the different compounds in OL-neuron co-cultures, while previous studies assessed myelination of OLs in the absence of neurons (Mei et al., 2014; Lee et al., 2012a; Kerman et al., 2015; Ou et al., 2016; Mogha et al., 2016).

This all-human neuron-OLs co-culture system allows to evaluate the effect of drugs on myelin expression, which should also allow modeling of pathways involved in neural diseases wherein OLs are involved, either because of defects in myelination or defects in neuronal support.

Finally, we demonstrated that induction of *SOX10* expression in NPCs following a single copy insertion of *SOX10* in a safe harbor locus of hPSCs (Ordovás et al., 2015) is sufficient to induce O4⁺ and MBP⁺ OL progeny. A similar methodology has recently been described by Pawlowski et al. (2017), who demonstrated that overexpression of *SOX10* and *OLIG2* induced cells with phenotypic features of OLs in a similar time frame as we demonstrate here, even though no functional characterization of the cells was performed. Generation of stable inducible *SOX10*-hPSC lines would be an invaluable tool for drug screens, as they do not suffer from random integrations and the incomplete efficiency of viral vectors, allowing a very efficient and robust generation of OLs.

In summary, we demonstrated that overexpression of only *SOX10* in hPSC-derived NPCs allows a very efficient and rapid generation of OLs from hPSCs, which can myelinate nude axons both *in vivo* and *in vitro* contexts. The protocol is robust, as it induces with similar efficiency

Figure 7. All hPSC-Derived OL-Neuron Co-culture Can Address Myelinating Drugs in an HTS Setting

(A) Relative MBP expression to control cultures (0.1% DMSO and no T3) of the different compounds and drugs affecting myelination: T3 (60 ng/mL), DAPT (1 μ M), miconazole (1 μ M), clobetasol propionate (5 μ M) and pranlukast (22.8 μ M). Three variables were assessed: total MBP⁺ area, number of MBP⁺ cells and total MBP⁺ intensity. Shown are results for co-cultures in 96-well plates, in 384-well plates, or the combination of the two.

(B) Gaussian dot plots of the average values of all single wells in the six culture conditions (N = 160 for all conditions except for pranlukast, where N = 90) for the three variables based on MBP expression.

(C) Representative images of the co-cultures assessing the effects of the different tested conditions on myelination and of the MBP⁺ mask identified for the analysis.

Hoechst 33258 (blue) was used as nuclear marker. Scale bars: 100 μ m. Data are represented as average values per plate \pm SEM of each condition of N = 7–8 independent experiments for 96-well plates, N = 6–7 for 384-well plates, and N = 12–15 for both 96- and 384-well plates. *p < 0.05, **p < 0.01.



and speed O4⁺ cells from hESCs and hiPSCs of healthy donors, as well as from hiPSCs from patients with MS or fALS. A platform was also developed wherein myelination of neurons can be evaluated in an HTS format to demonstrate the effect of myelinating factors and molecules. This all-hPSC-derived neuron-OL myelinating co-culture platform has the potential to significantly improve testing and validation of candidate pro-myelinating drugs for congenital or acquired demyelinating diseases, and allow assessment of mechanisms underlying neurodegenerative diseases wherein decreased OL-mediated neuronal support is fundamental to disease onset or progression.

EXPERIMENTAL PROCEDURES

Generation of NPCs and OLs from hPSCs

hPSCs were dissociated to single cells on day -2. On day 0, medium was switched to N2B27 medium supplemented with SB431542 10 μ M, LDN193189 1 μ M, and 100 nM RA until day 8, when SB431542 and LDN193189 were withdrawn and 1 μ M Smoothed agonist added. On day 12, cells were dissociated, plated, and transduced with viral vectors. Next day, medium was changed to OL differentiation medium with the addition of 1 μ g/mL doxycycline. Cells were maintained for 7–10 days.

Co-culture with Neurons and Adaptation for HTS

Cortical neurons were generated from WT hPSCs as described previously (Shi et al., 2012). Neuronal progenitors (~50 days) were replated and allowed to mature for 10–14 days. Afterward, purified O4⁺ cells were seeded above the maturing neurons and cultures were maintained for 20 days in co-culture medium in the absence of T3 and AA, with the addition of doxycycline and the presence of the candidate compounds.

Animal procedures (assessment of OL myelination in brain slices derived from shiverer mice) were approved by a Dutch Ethical Committee for animal experiments.

Detailed experimental procedures can be found in the [Supplemental Information](#).

ACCESSION NUMBERS

The transcriptome data reported in this paper have been deposited in the Gene Expression Omnibus under GEO: GSE106984.

SUPPLEMENTAL INFORMATION

Supplemental Information includes Supplemental Experimental Procedures, five figures, and seven tables and can be found with this article online at <https://doi.org/10.1016/j.stemcr.2017.12.014>.

AUTHOR CONTRIBUTIONS

J.A.G.L. and C.M.V. designed the project and experiments. J.A.G.L. performed most of the experiments and performed analysis of the data. M.K. helped with the co-cultures and HTS experiments and analysis. R.B. helped with generation of the endogenous SOX10-

expressing cell lines. D.C., J.O., and W.S.H. performed RNA-seq analysis. K.E. and P.B. helped with experiments regarding mRNA expression and immunostaining. E.W., J.C.D., and I.L. performed and analyzed the transmission electron microscopy experiments. N.G., F.d.V., B.L., and S.A.K. performed Shi^{-/-} mouse myelination assays. B.J. and N.C. helped in the analysis of the immunostainings. J.A.G.L. and C.M.V. wrote the manuscript. C.M.V. provided scientific guidance and support. All authors read the manuscript.

ACKNOWLEDGMENTS

We would like to acknowledge technical colleagues at SCIL (KU Leuven) for their technical support, Jonathan De Smedt for the heatmap representation of expression data, Prof. Fraser Sim (University of Buffalo, USA) for the MCS5-SOX10 reporter plasmids, Dr. Stefan Vinckier (Vesalius Research Center, VIB, KU Leuven, Belgium) for technical assistance with confocal microscopy, and Dr. John Pearson (Andalusian Center for Nanomedicine & Biotechnology, Spain) for 3D reconstruction of confocal microscopy images. J.A.G.L. has been supported by a Fellowship from the Alfonso Martín Escudero Foundation (Madrid, Spain) and M.K. by an H2020-MSCA-IF Fellowship. R.B. was funded by IWT/SB/121393 and S.A.K. by NWO-ZonMw Middelgroot (40-00506-98-10026). The work was supported by the IWT-iPSCAF grant (no. 150031) and the KUL-PF Stem Cells (no. PFO3) to C.M.V.

Received: May 9, 2017

Revised: December 15, 2017

Accepted: December 15, 2017

Published: January 11, 2018

REFERENCES

- Abiraman, K., Pol, S.U., O'Bara, M.A., Chen, G.D., Khaku, Z.M., Wang, J., Thorn, D., Vedia, B.H., Ekwegbalu, E.C., Li, J.X., et al. (2015). Anti-muscarinic adjunct therapy accelerates functional human oligodendrocyte repair. *J. Neurosci.* *35*, 3676–3688.
- Bilic, J., and Izpisua Belmonte, J.C. (2012). Concise review: induced pluripotent stem cells versus embryonic stem cells: close enough or yet too far apart? *Stem Cells* *30*, 33–41.
- Cahoy, J.D., Emery, B., Kaushal, A., Foo, L.C., Zamanian, J.L., Christopherson, K.S., Xing, Y., Lubischer, J.L., Krieg, P.A., Kruppenko, S.A., et al. (2008). A transcriptome database for astrocytes, neurons, and oligodendrocytes: a new resource for understanding brain development and function (2008). *J. Neurosci.* *28*, 264–278.
- Carey, B.W., Markoulaki, S., Hanna, J., Saha, K., Gao, Q., Mitalipova, M., and Jaenisch, R. (2009). Reprogramming of murine and human somatic cells using a single polycistronic vector. *Proc. Natl. Acad. Sci. USA* *106*, 157–162.
- Chambers, S.M., Fasano, C.A., Papapetrou, E.P., Tomishima, M., Sadelain, M., and Studer, L. (2009). Highly efficient neural conversion of human ES and iPS cells by dual inhibition of SMAD signaling. *Nat. Biotechnol.* *27*, 275–280.
- Deshmukh, V.A., Tardif, V., Lyssiotis, C.A., Green, C.C., Kerman, B., Kim, H.J., Padmanabhan, K., Swoboda, J.G., Ahmad, I., Kondo,



- T., et al. (2013). A regenerative approach to the treatment of multiple sclerosis. *Nature* 502, 327–332.
- Douvaras, P., and Fossati, V. (2015). Generation and isolation of oligodendrocyte progenitor cells from human pluripotent stem cells. *Nat. Protoc.* 10, 1143–1154.
- Douvaras, P., Wang, J., Zimmer, M., Hanchuk, S., O'Bara, M.A., Sadiq, S., Sim, F.J., Goldman, J., and Fossati, V. (2014). Efficient generation of myelinating oligodendrocytes from primary progressive multiple sclerosis patients by induced pluripotent stem cells. *Stem Cell Reports* 3, 250–259.
- Ehrlich, M., Mozafari, S., Glatza, M., Starost, L., Velychko, S., Hallmann, A.L., Cui, Q.L., Schambach, A., Kim, K.P., Bachelin, C., et al. (2017). Rapid and efficient generation of oligodendrocytes from human induced pluripotent stem cells using transcription factors. *Proc. Natl. Acad. Sci. USA* 114, E2243–E2252.
- Franklin, R.J., ffrench-Constant, C., Edgar, J.M., and Smith, K.J. (2012). Neuroprotection and repair in multiple sclerosis. *Nat. Rev. Neurol.* 8, 624–634.
- Furusho, M., Roulois, A.J., Franklin, R.J., and Bansal, R. (2015). Fibroblast growth factor signaling in oligodendrocyte-lineage cells facilitates recovery of chronically demyelinated lesions but is redundant in acute lesions. *Glia* 63, 1714–1728.
- Hu, B.Y., Du, Z.W., and Zhang, S.C. (2009). Differentiation of human oligodendrocytes from pluripotent stem cells. *Nat. Protoc.* 4, 1614–1622.
- Kerman, B.E., Kim, H.J., Padmanabhan, K., Mei, A., Georges, S., Joens, M.S., Fitzpatrick, J.A., Jappelli, R., Chandross, K.J., August, P., and Gage, F.H. (2015). In vitro myelin formation using embryonic stem cells. *Development* 142, 2213–2225.
- Lariosa-Willingham, K.D., Rosler, E.S., Tung, J.S., Dugas, J.C., Collins, T.L., and Leonoudakis, D. (2016). Development of a central nervous system axonal myelination assay for high throughput screening. *BMC Neurosci.* 17, 16.
- Lee, S., Leach, M.K., Redmond, S.A., Chong, S.Y., Mellon, S.H., Tuck, S.J., Feng, Z.Q., Corey, J.M., and Chan, J.R. (2012a). A culture system to study oligodendrocyte myelination processes using engineered nanofibers. *Nat. Methods* 9, 917–922.
- Lee, Y., Morrison, B.M., Li, Y., Lengacher, S., Farah, M.H., Hoffman, P.N., Liu, Y., Tsingalia, A., Jin, L., Zhang, P.W., et al. (2012b). Oligodendroglia metabolically support axons and contribute to neurodegeneration. *Nature* 487, 443–448.
- Marta, C.B., Adamo, A.M., Soto, E.F., and Pasquini, J.M. (1998). Sustained neonatal hyperthyroidism in the rat affects myelination in the central nervous system. *J. Neurosci. Res.* 53, 251–259.
- Marques, S., Zeisel, A., Codeluppi, S., van Bruggen, D., Mendanha Falcão, A., Xiao, L., Li, H., Häring, M., Hochgerner, H., Romanov, R.A., et al. (2016). Oligodendrocyte heterogeneity in the mouse juvenile and adult central nervous system. *Science* 352, 1326–1329.
- Mei, F., Fancy, S.P., Shen, Y.A., Niu, J., Zhao, C., Presley, B., Miao, E., Lee, S., Mayoral, S.R., Redmond, S.A., et al. (2014). Micropillar arrays as a high-throughput screening platform for therapeutics in multiple sclerosis. *Nat. Med.* 20, 954–960.
- Mogha, A., D'Rozario, M., and Monk, K.R. (2016). G protein-coupled receptors in myelinating glia. *Trends Pharmacol. Sci.* 37, 977–987.
- Najm, F.J., Lager, A.M., Zaremba, A., Wyatt, K., Caprariello, A.V., Factor, D.C., Karl, R.T., Maeda, T., Miller, R.H., and Tesar, P.J. (2013). Transcription factor-mediated reprogramming of fibroblasts to expandable, myelinogenic oligodendrocyte progenitor cells. *Nat. Biotechnol.* 31, 426–433.
- Najm, F.J., Madhavan, M., Zaremba, A., Shick, E., Karl, R.T., Factor, D.C., Miller, T.E., Nevin, Z.S., Kantor, C., Sargent, A., et al. (2015). Drug-based modulation of endogenous stem cells promotes functional remyelination in vivo. *Nature* 522, 216–220.
- Nielsen, J.A., Maric, D., Lau, P., Barker, J.L., and Hudson, L.D. (2006). Identification of a novel oligodendrocyte cell adhesion protein using gene expression profiling. *J. Neurosci.* 26, 9881–9891.
- Nistor, G.I., Totoiu, M.O., Haque, N., Carpenter, M.K., and Keirstead, H.S. (2005). Human embryonic stem cells differentiate into oligodendrocytes in high purity and myelinate after spinal cord transplantation. *Glia* 49, 385–396.
- Ordovás, L., Boon, R., Pistoni, M., Chen, Y., Wolfs, E., Guo, W., Sambathkumar, R., Bobis-Wozowicz, S., Helsen, N., Vanhove, J., et al. (2015). Efficient recombinase-mediated cassette exchange in hPSCs to study the hepatocyte lineage reveals AAVS1 locus-mediated transgene inhibition. *Stem Cell Reports* 5, 918–931.
- Ou, Z., Sun, Y., Lin, L., You, N., Liu, X., Li, H., Ma, Y., Cao, L., Han, Y., Liu, M., et al. (2016). Olig2-targeted G-protein-coupled receptor Gpr17 regulates oligodendrocyte survival in response to lysolecithin-induced demyelination. *J. Neurosci.* 36, 10560–10573.
- Pawlowski, M., Ortmann, D., Bertero, A., Tavares, J.M., Pedersen, R.A., Vallier, L., and Kotter, M.R.N. (2017). Inducible and deterministic forward programming of human pluripotent stem cells into neurons, skeletal myocytes, and oligodendrocytes. *Stem Cell Reports* 8, 803–812.
- Pol, S.U., Lang, J.K., O'Bara, M.A., Cimato, T.R., McCallion, A.S., and Sim, F.J. (2013). Sox10-MCS5 enhancer dynamically tracks human oligodendrocyte progenitor fate. *Exp. Neurol.* 247, 694–702.
- Pozniak, C.D., Langseth, A.J., Dijkgraaf, G.J., Choe, Y., Werb, Z., and Pleasure, S.J. (2010). Sox10 directs neural stem cells toward the oligodendrocyte lineage by decreasing suppressor of fused expression. *Proc. Natl. Acad. Sci. USA* 107, 21795–21800.
- Shi, Y., Kirwan, P., Smith, J., Robinson, H.P., and Livesey, F.J. (2012). Human cerebral cortex development from pluripotent stem cells to functional excitatory synapses. *Nat. Neurosci.* 15, 477–486, S1.
- Sim, F.J., McClain, C.R., Schanz, S.J., Protack, T.L., Windrem, M.S., and Goldman, S.A. (2011). CD140a identifies a population of highly myelinogenic, migration-competent and efficiently engrafting human oligodendrocyte progenitor cells. *Nat. Biotechnol.* 29, 934–941.
- Sommer, I., and Schachner, M. (1981). Monoclonal antibodies (O1 to O4) to oligodendrocyte cell surfaces: an immunocytological study in the central nervous system. *Dev. Biol.* 83, 311–327.
- Vogl, M.R., Reiprich, S., Küspert, M., Kosian, T., Schrewe, H., Nave, K.A., and Wegner, M. (2013). Sox10 cooperates with the mediator subunit 12 during terminal differentiation of myelinating glia. *J. Neurosci.* 33, 6679–6690.



- Wang, S., Bates, J., Li, X., Schanz, S., Chandler-Militello, D., Levine, C., Maherali, N., Studer, L., Hochedlinger, K., Windrem, M., and Goldman, S.A. (2013). Human iPSC-derived oligodendrocyte progenitor cells can myelinate and rescue a mouse model of congenital hypomyelination. *Cell Stem Cell* 12, 252–264.
- Wegner, M. (2010). All purpose Sox: the many roles of Sox proteins in gene expression. *Int. J. Biochem. Cell Biol.* 42, 381–390.
- Weider, M., Reiprich, S., and Wegner, M. (2013). Sox appeal—Sox10 attracts epigenetic and transcriptional regulators in myelinating glia. *Biol. Chem.* 394, 1583–1593.
- Weider, M., and Wegner, M. (2017). SoxE factors: transcriptional regulators of neural differentiation and nervous system development. *Semin. Cell Dev. Biol.* 63, 35–42.
- Weng, Q., Chen, Y., Wang, H., Xu, X., Yang, B., He, Q., Shou, W., Chen, Y., Higashi, Y., van den Berghe, V., et al. (2012). Dual-mode modulation of Smad signaling by Smad-interacting protein Sip1 is required for myelination in the central nervous system. *Neuron* 73, 713–728.
- Yang, N., Zuchero, J.B., Ahlenius, H., Marro, S., Ng, Y.H., Vierbuchen, T., Hawkins, J.S., Geissler, R., Barres, B.A., and Wernig, M. (2013). Generation of oligodendroglial cells by direct lineage conversion. *Nat. Biotechnol.* 31, 434–439.
- Zawadzka, M., Rivers, L.E., Fancy, S.P., Zhao, C., Tripathi, R., Jamen, F., Young, K., Goncharevich, A., Pohl, H., Rizzi, M., et al. (2010). CNS-resident glial progenitor/stem cells produce Schwann cells as well as oligodendrocytes during repair of CNS demyelination. *Cell Stem Cell* 6, 578–590.
- Zhang, Y., Chen, K., Sloan, S.A., Bennett, M.L., Scholze, A.R., O’Keeffe, S., Phatnani, H.P., Guarnieri, P., Caneda, C., Ruderisch, N., et al. (2014). An RNA-sequencing transcriptome and splicing database of glia, neurons, and vascular cells of the cerebral cortex. *J. Neurosci.* 34, 11929–11947.
- Zhang, Y., Sloan, S.A., Clarke, L.E., Caneda, C., Plaza, C.A., Blumenthal, P.D., Vogel, H., Steinberg, G.K., Edwards, M.S., Li, G., et al. (2016). Purification and characterization of progenitor and mature human astrocytes reveals transcriptional and functional differences with mouse. *Neuron* 89, 37–53.

Stem Cell Reports, Volume 10

Supplemental Information

SOX10 Single Transcription Factor-Based Fast and Efficient Generation of Oligodendrocytes from Human Pluripotent Stem Cells

Juan Antonio García-León, Manoj Kumar, Ruben Boon, David Chau, Jennifer One, Esther Wolfs, Kristel Eggermont, Pieter Berckmans, Nilhan Gunhanlar, Femke de Vrij, Bas Lendemeijer, Benjamin Pavie, Nikky Corthout, Steven A. Kushner, José Carlos Dávila, Ivo Lambrechts, Wei-Shou Hu, and Catherine M. Verfaillie

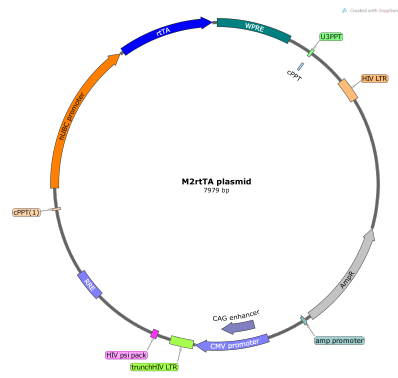
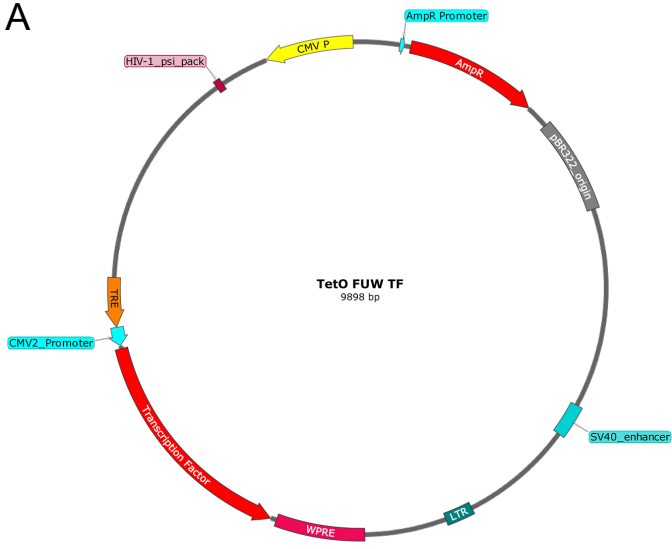
SOX10 Single Transcription Factor Based Fast and Efficient Generation of Oligodendrocytes from Human Pluripotent Stem Cells

Juan Antonio García-León^{1,*}, Manoj Kumar¹, Ruben Boon¹, David Chau², Jennifer One², Esther Wolfs³, Kristel Eggermont¹, Pieter Berckmans¹, Nilhan Gunhanlar⁴, Femke de Vrij⁴, Bas Lendemeijer⁴, Benjamin Pavie⁵, Nikky Corthout⁵, Steven A Kushner⁴, José Carlos Dávila⁶, Ivo Lambrichts³, Wei-Shou Hu² & Catherine M Verfaillie^{1,*}

Inventory of Supplemental Information:

- Supplementary Figures 1-5
- Supplementary Figure Legends
- Supplementary Table 1 (.xls)
- Supplementary Table 2 (.xls)
- Supplementary Tables 3-7
- Supplementary Experimental Procedures
- Supplementary Experimental Procedure References

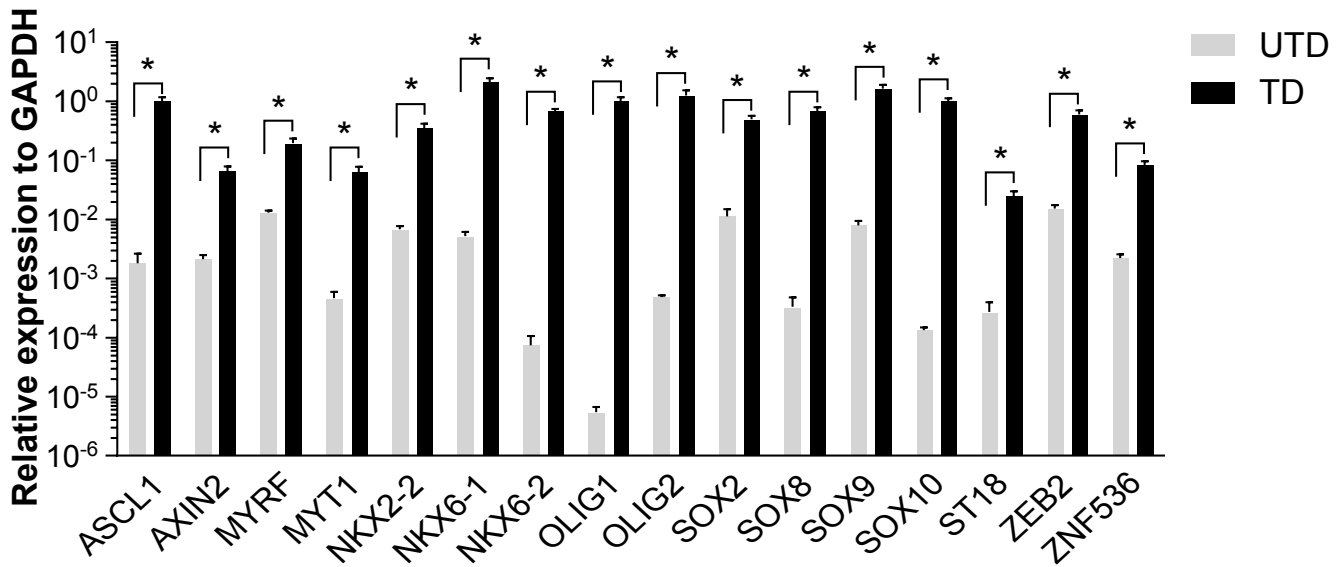
A



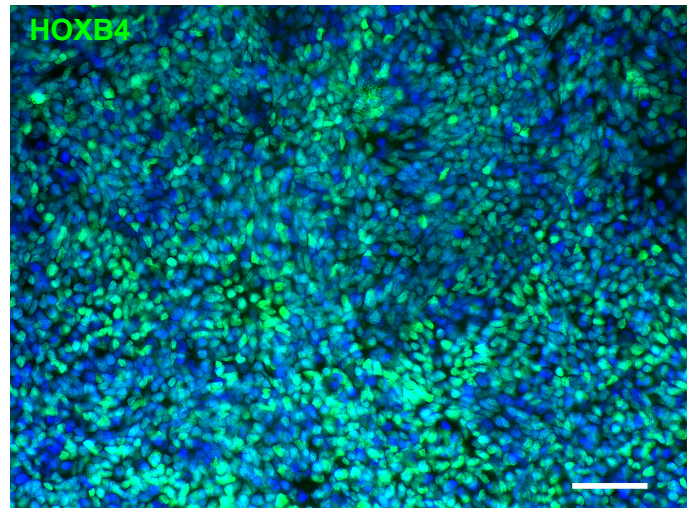
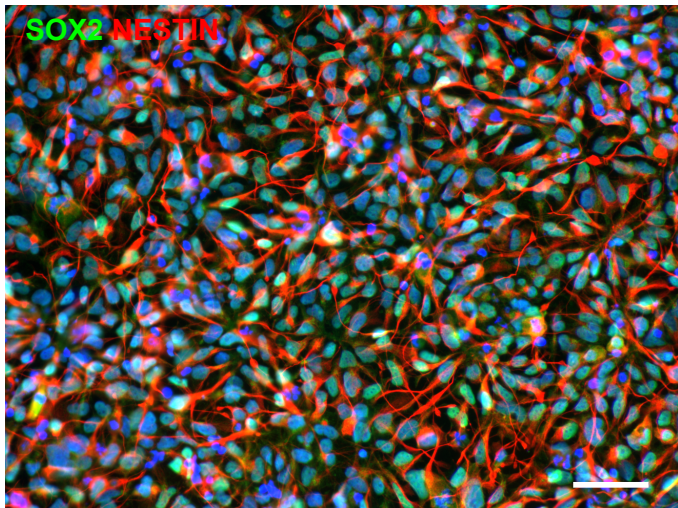
TF selected

ASCL, AXIN2, MYRF, MYT1, NKX2-2, NKX6-1, NKX6-2, OLIG1, OLIG2, SOX2, SOX8, SOX9, SOX10, ST18, ZEB2, ZNF536

B



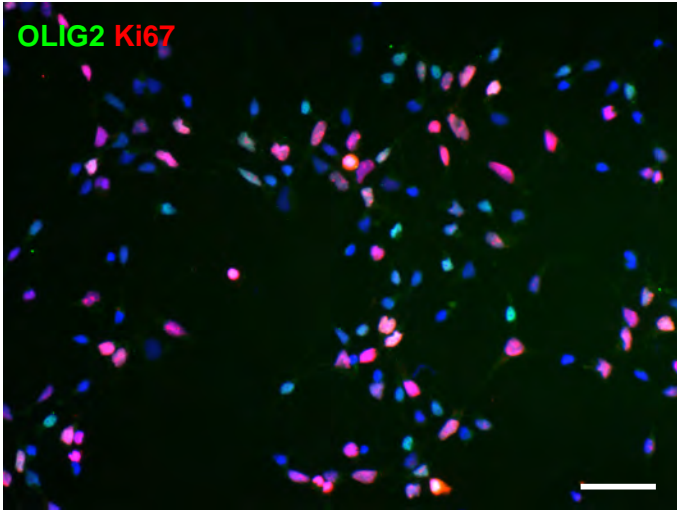
C



Day 0

A

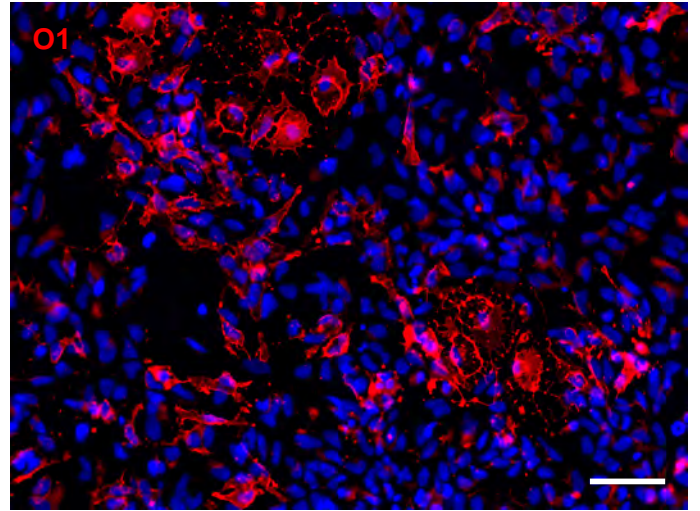
OLIG2 Ki67



Day 10

B

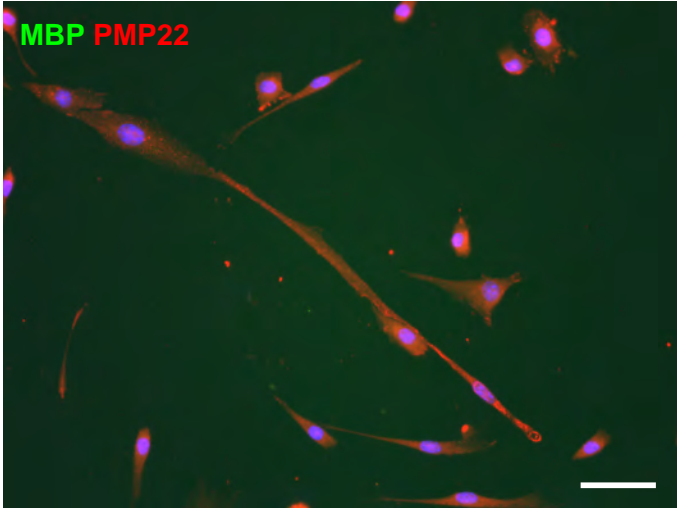
O1



Primary murine Schwann cells

C

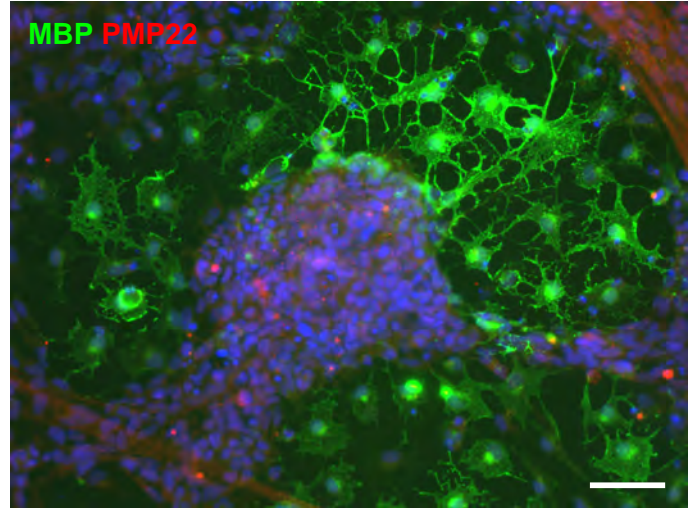
MBP PMP22



SOX10-transduced cells Day 10

D

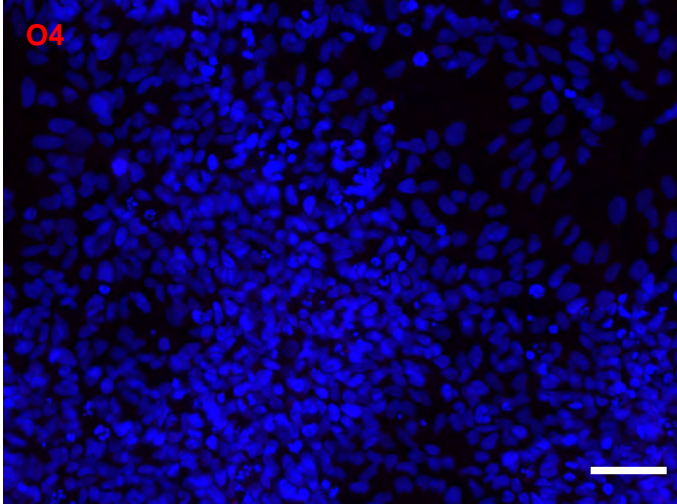
MBP PMP22



eGFP-transduced cells Day 10

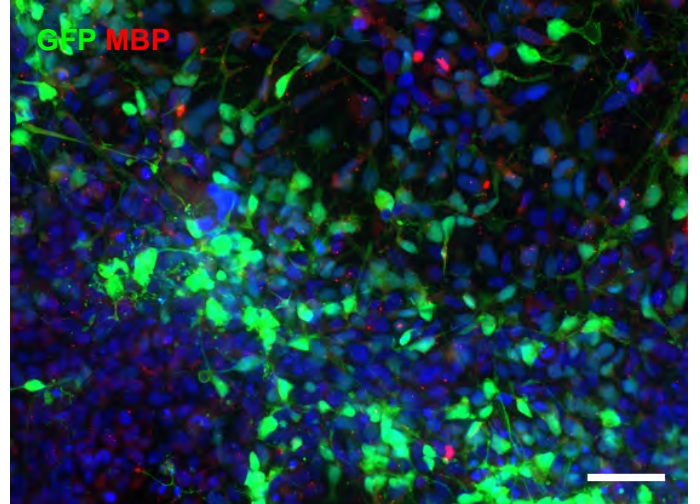
E

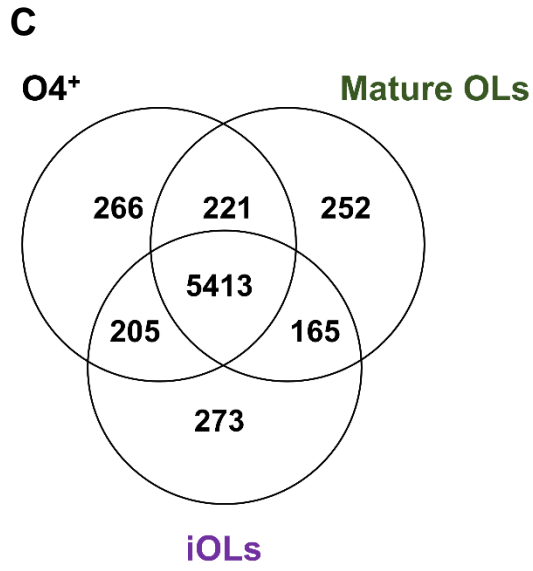
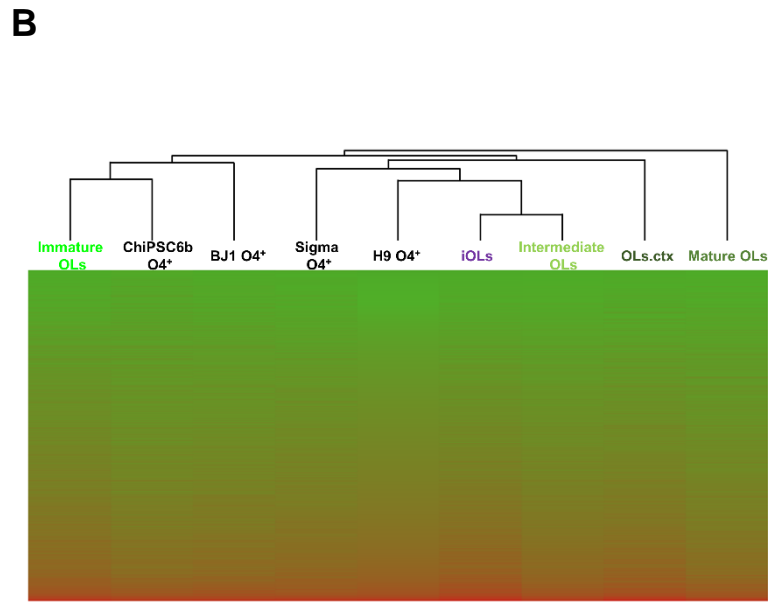
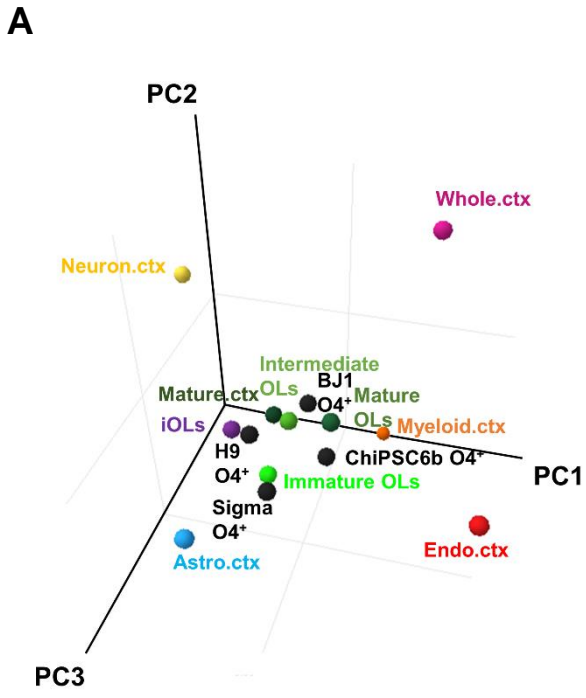
O4



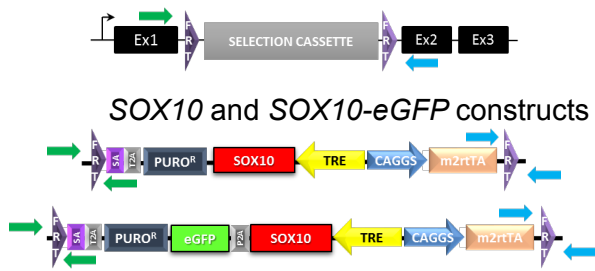
F

GFP MBP

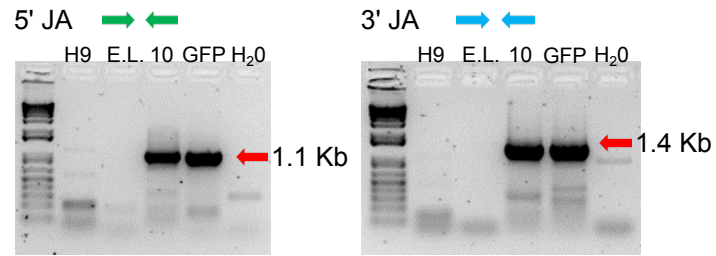




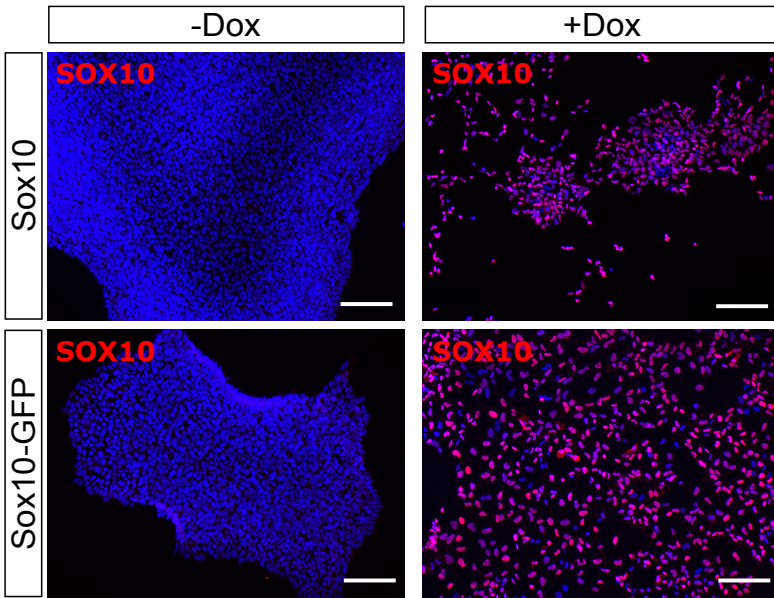
A Engineered hPSC line: *PPP1R12C* AAVS1 locus



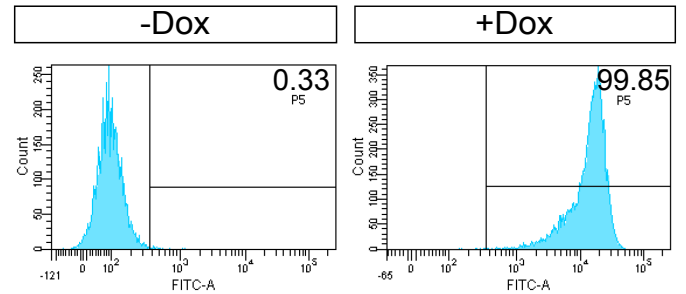
B



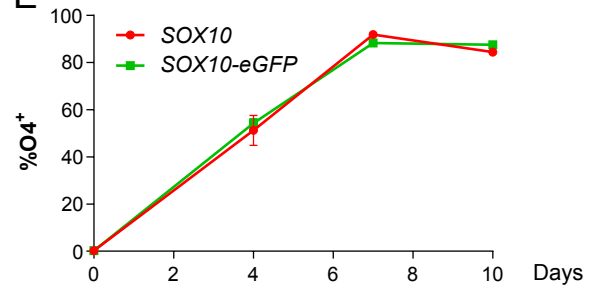
C



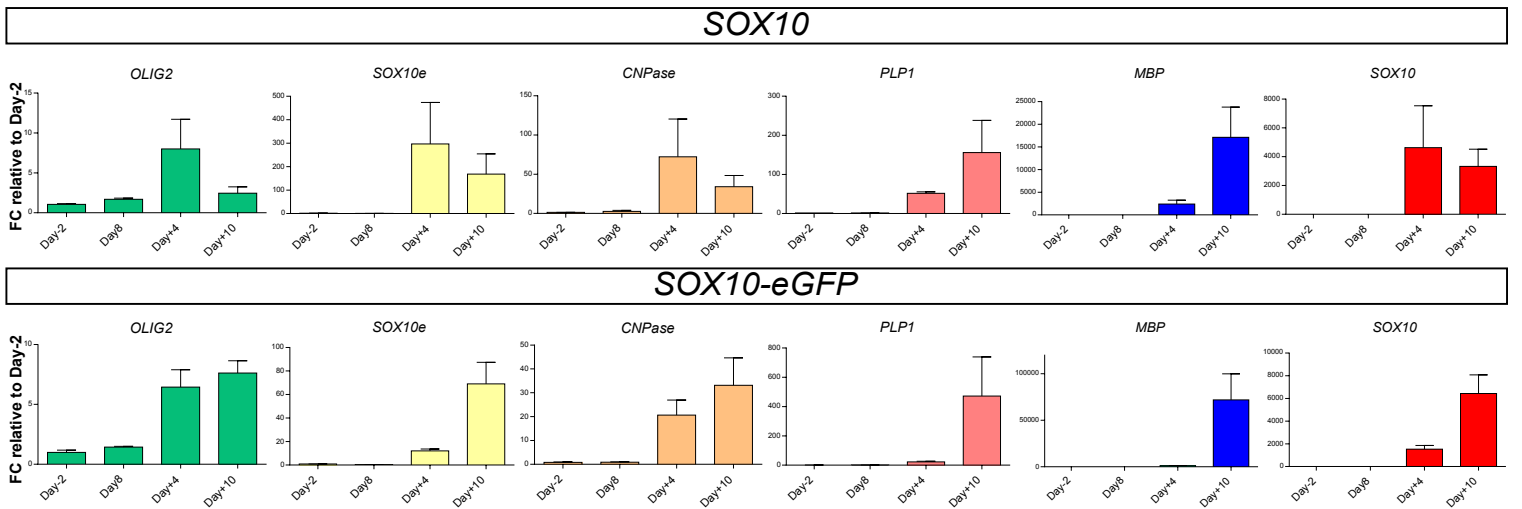
D



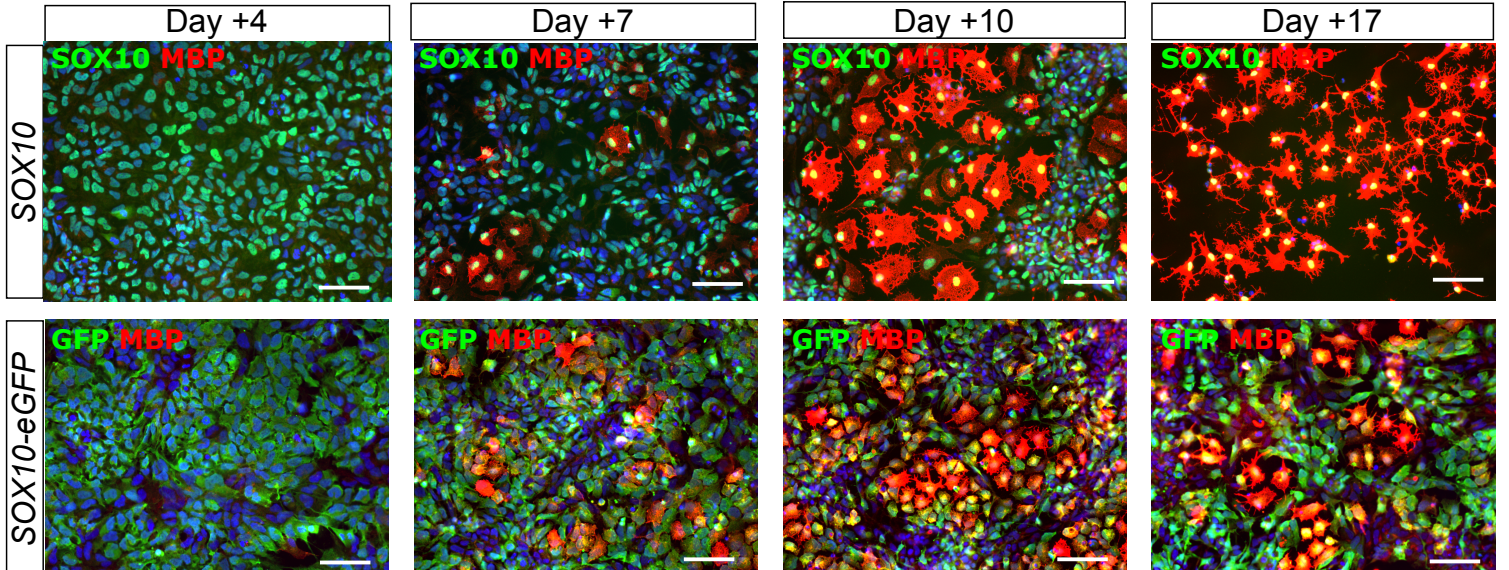
E



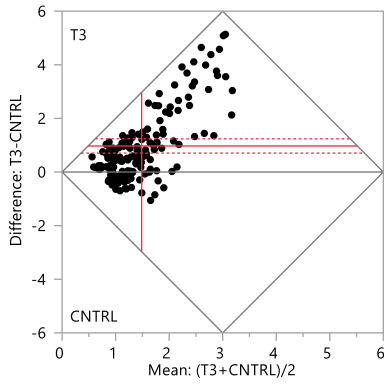
F



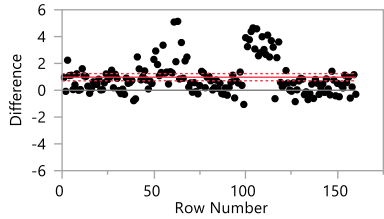
G



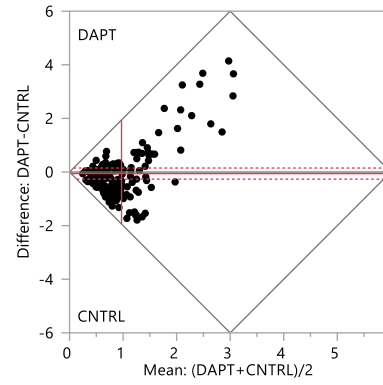
Difference: T3-CNTRL



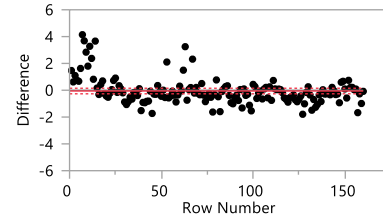
| | |
|-----------------|---------|
| T3 | 1.97218 |
| CNTRL | 1.00 |
| Mean Difference | 0.97218 |
| Std Error | 0.10229 |
| Upper 99% | 1.23886 |
| Lower 99% | 0.70552 |
| N | 160 |
| Correlation | -0.0647 |
| Prob > t | <.0001* |
| Prob > t | <.0001* |
| Prob < t | 1.0000 |



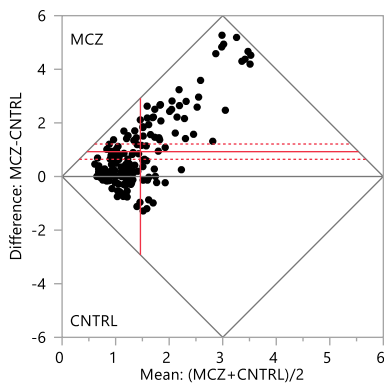
Difference: DAPT-CNTRL



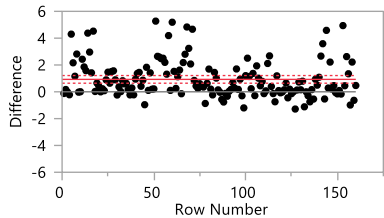
| | |
|-----------------|---------|
| DAPT | 0.94134 |
| CNTRL | 1.00 |
| Mean Difference | -0.0587 |
| Std Error | 0.07965 |
| Upper 99% | 0.14901 |
| Lower 99% | -0.2663 |
| N | 160 |
| Correlation | 0.13922 |
| Prob > t | 0.4626 |
| Prob > t | 0.7687 |
| Prob < t | 0.2313 |



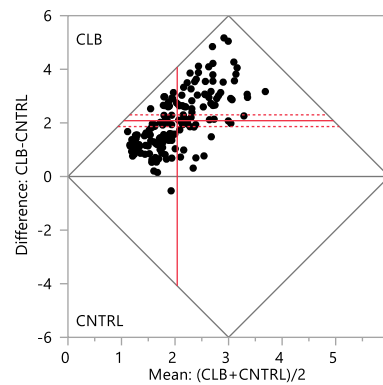
Difference: MCZ-CNTRL



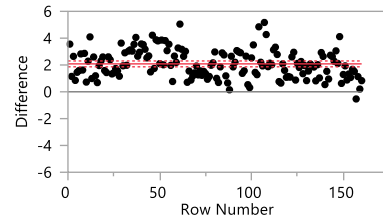
| | |
|-----------------|---------|
| MCZ | 1.92664 |
| CNTRL | 1.00 |
| Mean Difference | 0.92664 |
| Std Error | 0.10953 |
| Upper 99% | 1.21222 |
| Lower 99% | 0.64109 |
| N | 160 |
| Correlation | -0.0754 |
| Prob > t | <.0001* |
| Prob > t | <.0001* |
| Prob < t | 1.0000 |



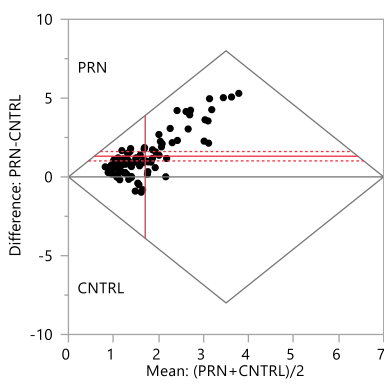
Difference: CLB-CNTRL



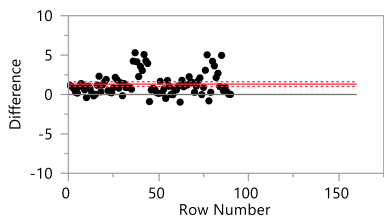
| | |
|-----------------|---------|
| CLB | 3.08201 |
| CNTRL | 1.00 |
| Mean Difference | 2.08201 |
| Std Error | 0.08382 |
| Upper 99% | 2.30056 |
| Lower 99% | 1.86349 |
| N | 160 |
| Correlation | 0.07246 |
| Prob > t | <.0001* |
| Prob > t | <.0001* |
| Prob < t | 1.0000 |



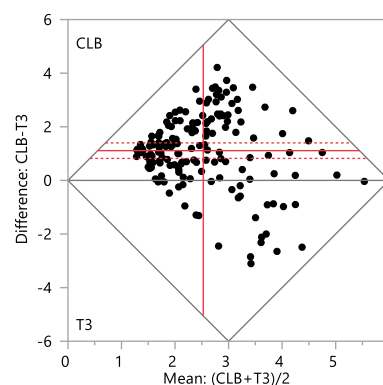
Difference: PRN-CNTRL



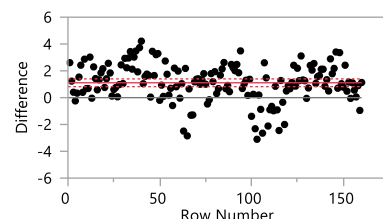
| | |
|-----------------|---------|
| PRN | 2.36116 |
| CNTRL | 1.00 |
| Mean Difference | 1.36116 |
| Std Error | 0.1497 |
| Upper 99% | 1.61004 |
| Lower 99% | 1.01514 |
| N | 90 |
| Correlation | -0.0319 |
| Prob > t | <.0001* |
| Prob > t | <.0001* |
| Prob < t | 1.0000 |



Difference: CLB-T3



| | |
|-----------------|---------|
| CLB | 3.08201 |
| T3 | 1.97218 |
| Mean Difference | 1.10983 |
| Std Error | 0.11095 |
| Upper 99% | 1.39909 |
| Lower 99% | 0.82058 |
| N | 160 |
| Correlation | 0.18061 |
| Prob > t | <.0001* |
| Prob > t | <.0001* |
| Prob < t | 1.0000 |



SUPPLEMENTARY FIGURE LEGENDS

Supplementary Figure 1. Lentiviral inducible overexpression system used for the initial screening with 16 TFs, and characterization of NPCs. Related to Figure 1.

(A) Scheme of the lentiviral vector system used for the overexpression of the 16 TFs selected. (B) Expression levels of each TF in untransduced (UTD) vs. transduced (TD) conditions. (C) Phenotypic characterization of NPCs generated for the transduction with each TF. Gene expression levels normalized to *GAPDH*. Hoechst 33258 (blue) was used as nuclear marker. Scale bar: 50 μm . Data is represented as Mean \pm SEM of N=3 independent experiments. * $p < 0.05$.

Supplementary Figure 2. Phenotypic characterization of OPC/OLs generated by *SOX10* overexpression. Related to Figure 3.

(A) Immunostaining for the early OPC marker OLIG2 and Ki67 proliferation marker in NPCs before transduction. (B) Immunostaining for the ganglioside marker O1 in *SOX10*-induced cells. (C-D) Generated OPC/OLs are morphologically different from Schwann cells (SCs) and do not express typical SC markers. (C) Primary Schwann cells obtained from postnatal murine tissue express PMP22 but not MBP. (D) *SOX10*-induced OPC/OLs do not express the Schwann cell marker PMP22. No expression of O4 (E) or MBP (F) is observed for *eGFP*-transduced NPCs after 10 days of induction. Hoechst 33258 (blue) was used as nuclear marker. Scale bar: 50 μm .

Supplementary Figure 3. Global transcriptome comparison of *SOX10*-induced O4⁺ cells (derived from H9, ChiPSC6b, Sigma-IPSC0028 and BJ1 PSC lines, n=12) with different samples including TF-induced human OLs from the study of Ehrlich *et al.* (Ehrlich *et al.*, 2017). Related to Figure 4.

(A) Principal component analysis (PCA) of the different samples analyzed. (B) Hierarchical clustering of whole-genome expression profile of *SOX10*-induced O4⁺ cells (black), different primary OL samples (green), and iOLs from Ehrlich *et al.* (purple). (C) Differentially expressed genes identified from sequence alignment map (SAM) using FDR ≤ 0.05 and >2 fold change among PSC-O4⁺ cells, primary mature OLs and iOLs.

Supplementary Figure 4. Generation of hPSC lines endogenously overexpressing the *SOX10* TF.

(A) Schemes of the targeting of the endogenous *AAVS1* locus and of the constructs created for inducible overexpression of *SOX10*. (B) 5' and 3' junction assay (JA) PCRs to check for the insertion of *SOX10* and *SOX10-eGFP*-containing selection cassettes at correct genomic location and graphical depiction of the primers used (H9: untargeted cells, E.L.: engineered line with selection cassette inserted in *AAVS1* locus, 10: engineered line with *SOX10*-expressing cassette inserted, GFP: engineered line with *SOX10-eGFP*-expressing cassette inserted). (C) Doxycycline inducible expression of *SOX10* in both lines generated. (D) Doxycycline inducible expression of GFP after successful generation of the *SOX10-GFP* line measured by FACS. (E) O4 expression along the days after doxycycline induction in both *SOX10* and *SOX10-GFP* lines. (F) Gene expression levels of OPC/OL markers along the days in both *SOX10* and *SOX10-GFP* lines. *SOX10e* is referred to the endogenous expression of this gene. Gene expression levels normalized to *GAPDH*. (G) Representative images of the phenotypic characterization performed along differentiation of both lines. Hoechst 33258 (blue) was used as nuclear marker. Scale bar: 50 μm . Data is represented as Mean \pm SEM of N=3 independent experiments. * $p < 0.05$.

Supplementary Figure 5. Results of matched-pair analysis of the total area identified as MBP⁺ expression (MBP⁺ area) relative to control condition (0.1% DMSO) of the different tested compounds/drugs affecting myelination. Related to Figure 7.



The results show differences in MBP⁺ area of the tested compound compared to control condition (N=160 for all conditions except for pranlukast, where N=90). For each comparison, the first graph is the difference plot which shows the mean of each response, the difference of the means (shown as the horizontal line), and the 95% confidence interval (above and below shown as dotted lines). The mean of pairs is shown by the vertical line. The second graph is the Tukey mean-difference plot and represents the differences by each row of the comparison. The following comparisons were performed: (A) T3-control, (B) DAPT-control, (C) Miconazole (MCZ)-control, (D) Clobetasol propionate (CLB)-control and (E) Pranlukast (PRN)-control. As can be observed, all compounds showed significant higher expression of MBP⁺ area compared to control except DAPT. Comparison of all compounds among themselves was also performed, with Clobetasol propionate (CLB) being the only one showing significant higher MBP⁺ expression compared to T3 (F) ($p = 0.0001$; paired t test). $P < 0.05$ (Prob > |t|) indicates difference is statistically significant.

Supplementary Table 3: List of primer sequences used for PCR amplification of the CDS of the selected transcription factors for cloning into the FUW lentiviral vector.

| Genes | Primer sequences (5' to 3') | Type |
|--------|--|---------|
| ASCL1 | cgatt <u>GAATTC</u> ATGGAAAGCTCTGCCAAGAT | Forward |
| | cgattGAATTCAGAACCGATTGGTGAAGTC | Reverse |
| AXIN2 | gtacgCAATTGATGAGTAGCGCTATGTTGGTGAC | Forward |
| | gtacgCAATTGTCAATCGATCCGCTCCAC | Reverse |
| MYRF | cagcaCAATTGATGCACTGGCTTCCAGCA | Forward |
| | tgaaCAATTGTCAGTCACACAGGCGGTAGAAGT | Reverse |
| MYT1 | gtatcGAATTCATGAGCTTAGAAAATGAAGACAAGC | Forward |
| | gtatcGAATTCCTAGACCTGGATGCCCTC | Reverse |
| NKX2-2 | tcagtGAATTCATGTCGCTGACCAACACAAA | Forward |
| | tcagtGAATTCACCAAGTCCACTGCTGG | Reverse |
| NKX6-1 | tactgGAATTCATGTTAGCGGTGGGGGCAAT | Forward |
| | tactgGAATTCAGGATGAGCTCTCCGGCT | Reverse |
| NKX6-2 | tcagaGAATTCATGGACACTAACCGCCCG | Forward |
| | tcagaGAATTCACAAAGGCGTCCCCCG | Reverse |
| OLIG1 | tacgtGAATTCATGTAATCTATGCGGTTTCCCAG | Forward |
| | tacgtGAATTCCTACTTGGAGAATTGCGC | Reverse |
| OLIG2 | tcaagGAATTCATGGACTCGGACGCCAG | Forward |
| | tcaagGAATTCCTACTTGGCGTCGGAGG | Reverse |
| SOX2 | gatcgGAATTCATGTACAACATGATGGAGACGGA | Forward |
| | gatcgGAATTCACATGTGTGAGAGGGGC | Reverse |
| SOX8 | gttcaGAATTCATGCTGGACATGAGCGAGG | Forward |
| | gttcaGAATTCAGGGCCTGGTCAGGGT | Reverse |
| SOX9 | tagctGAATTCATGAATCTCTGGACCCCTT | Forward |
| | tagctGAATTCCTCAAGGTGAGTGAGCTGTG | Reverse |
| SOX10 | catgaGAATTCATGGCGGAGGAGCAGGAC | Forward |
| | catgaGAATTCCTAGGGCCGGGACAGTGTC | Reverse |
| ST18 | gtcaaGAATTCATGGATGCAGAGGCTGAAGA | Forward |
| | gtcaaGAATTCCTACACATGGATACCCTTCACTGC | Reverse |
| ZEB2 | agcaCAATTGATGAAGCAGCCGATCATGGC | Forward |
| | tgaaCAATTGTTACATGCCATCTCCATATTGTCTTCC | Reverse |
| ZNF536 | gatcgGAATTCATGGAAGAAGCGAGCCTGTGCCTT | Forward |
| | gatcgGAATTCCTACTTACCACACAAGTCTGGCCTCTTG | Reverse |
| eGFP | TAGTGAATTCATGGTGAAGCAAGGGCGAG | Forward |
| | TAGTGAATTCCTACTTGTACAGCTCGTCCATGC | Reverse |

*The underlined sequences denote the EcoRI restriction sites. For MYRF,ZEB2 and AXIN2, MfeI restriction sites were used.

Supplementary Table 4: List of primers and conditions used for junction assay PCRs.

| Symbol | Target | Amp. size | Sequence | Orientation | PCR Protocol |
|---|--------|-----------|------------------------|-------------|---|
|  | 5' JA | 1028 bp | CACTTTGAGCTCTACTGGCTTC | Forward | 95 °C/5 min, [95 °C/30 sec, 68 °C (-0.5 °C/cycle) /90 sec] x 15, [95 °C/30 sec, 58 °C/30 sec, 72 °C/90 sec] x 25, 72 °C/5 min |
| | | | CATGTTAGAAGACTTCCTCTGC | Reverse | |
|  | 3' JA | 1384 bp | ACCTTGATATGCTGCCTGCT | Forward | |
| | | | AAGGCAGCCTGGTAGACA | Reverse | |

Supplementary Table 5: List of primer sequences used for gene expression analysis by QPCR.

| Genes | Primer sequences (5' to 3') | Type |
|---------------|-----------------------------|---------|
| ASCL1 | CCCCCAACTACTCCAACGAC | Forward |
| | TGAAGTCGAGAAGCTCCTGC | Reverse |
| AXIN2 | TCATTTCCCGAGAACCCACC | Forward |
| | TCGGAGCCCTCTCTCTTC | Reverse |
| MYRF | TAACTACAAGGAGCTGCCCATG | Forward |
| | TGGTTCTTCTTCTGGCACAC | Reverse |
| MYT1 | AAGAGCTGAGAAGCGTGAGATC | Forward |
| | CATGCATGGCTAAGATCTCTGG | Reverse |
| NKX2-2 | GAACCCCTTCTACGACAGCA | Forward |
| | AGACCGTGCAGGGAGTACT | Reverse |
| NKX6-1 | CCATCTTCTGGCCCGGAGTGA | Forward |
| | CTTCCCGTCTTTGTCCAACAA | Reverse |
| NKX6-2 | CCAGGTGAAGGTCTGGTTCC | Forward |
| | GTATTCGTCGTCGTCTCCG | Reverse |
| OLIG1 | GCATGCAGGACCTGAACCT | Forward |
| | TATCTTGGAGAGCTTGCGGC | Reverse |
| OLIG2 | GACAAGCTAGGAGGCAGTGG | Forward |
| | TCCGGCTCTGTCATTTGCTT | Reverse |
| SOX2 | GAGTGGAACCTTTTGTGGAGA | Forward |
| | AGCGTGTACTTATCCTTCTTCAT | Reverse |
| SOX8 | CCCGACTACAAGTACCAGCC | Forward |
| | GGTCTGCCCTGTGTGGTC | Reverse |
| SOX9 | GAACAAGCCGCACGTCAAG | Forward |
| | TCGCTCTCGTTCAGAAGTCTC | Reverse |
| SOX10 | CTTCATGGTGTGGGCTCAGG | Forward |
| | CACTTTCGTTTCAGCAGCCTC | Reverse |
| ST18 | CTCTACCGCAGAGGAAATCATG | Forward |
| | AAGACTTGACCATGAGCTCTTG | Reverse |
| ZEB2 | AGGGACAGATCAGCACCAAATG | Forward |
| | GGGCACTCGTAAGGTTTTTCAC | Reverse |
| ZNF536 | ATGAAGGACTGCCCCGACTG | Forward |
| | GGTTTCTCACCTGTGTGTATCC | Reverse |
| GAPDH | TCAAGAAGGTGGTGAAGCAGG | Forward |
| | ACCAGGAAATGAGCTTGACAAA | Reverse |
| Sox2e | TGGCGAACCATCTCTGTGGT | Forward |
| | CCAACGGTGTCAACCTGCAT | Reverse |
| Olig2e | CACAGAGCAGTGGGGAGTG | Forward |
| | GCACACAGCGGTACCTTTTC | Reverse |
| Ascl1e | GAGCAACTGGGACCTGAGTC | Forward |
| | TCAGCTGTGCGTGTAGAGG | Reverse |
| Sox10e | TTCTGAAGGCAGGAAGGAGTTG | Forward |
| | ATGCGTCTCAAGGTCATGGAG | Reverse |
| CSPG4 | TCAGGCAGAGGTCTACGCT | Forward |
| | TAGGGTATCATGGGCCTCCC | Reverse |
| GalC | TGTCGTGACCTGGATTGTGG | Forward |
| | TGACCTCTCATTCCAAATTCCA | Reverse |
| MBP | AGGCAGAGCGTCCGACTATA | Forward |
| | CGACTATCTTCTCCAGC | Reverse |
| CNPase | ATGGTCAGCGTGAAGGC | Forward |
| | CAACCAAGTTTTGTGACTACGG | Reverse |

| | | |
|--------------|-------------------------|---------|
| PLP1 | GGTTCCCTGCTCACCTTCA | Forward |
| | TCAGAACTTGGTGCCTCGG | Reverse |
| OMG | GTGCATATACATTGGAGAGGACA | Forward |
| | AGATGCTGATGTTGAAGACGA | Reverse |
| MOBP | GTGTTCCGAGTACTTCTGGTT | Forward |
| | GCAAATGATACCAAGACAAGCTC | Reverse |
| GPR17 | GATGAAGTCGTTGAGTGTCTAGG | Forward |
| | CAGATGCCACCATTTCTCTA | Reverse |

*Those genes followed by *e* denotes primers designed to distinguish endogenous from transgene expression of a certain factor.

Supplementary Table 6: List of primary antibodies used for immunostainings.

| Antigen | Dilution | Host and serotype | Reference |
|-----------------------|------------------------------|---------------------|-----------------------------|
| A2B5 | 1/500 | Mouse IgM | Millipore MAB312 |
| O4-APC (FACS) | 1/20 | Mouse IgM | Miltenyi 130-095-891 |
| O4 (immunostaining) | 1/300 | Mouse IgM | R&D MAB1326 |
| O1 | 1/300 | Mouse IgM | R&D MAB1327 |
| Olig2 | 1/100 | Goat polyclonal IgG | Santa cruz SC-19969 |
| MBP | 1/75 1/200 (brain slices) | Chicken IgY | Millipore AB9348 |
| MOG | 1/100 | Mouse IgG1 | Millipore MAB 5680 |
| PLP | 1/100 | Rabbit IgG | Abcam ab28486 |
| hNA | 1/200 | Mouse IgG1 | Millipore MAB1281 |
| NF200 | 1/200 | Rabbit IgG | Sigma N4142 |
| TUJ1 (beta 3 tubulin) | 1/1000 | Rabbit polyclonal | Synaptic systems 302302 |
| SOX10 | 1/100 | Goat polyclonal IgG | R&D AF 2864 |
| Ki67 | 1/200 | Mouse IgG1 | BD 556003 |
| SOX2 | 1/200 | Rabbit IgG | Millipore Ab5603 |
| NESTIN | 1/200 | Mouse IgG1 | Covance 656802 |
| HOXB4 | 1/50 | Rat IgG | DSHB 112 anti-Hoxb4 |
| PMP22 | 1/100 | Rabbit IgG | Novus biotechnie NBP1-67670 |
| GFP | 1/500 | Goat IgG | Abcam ab5450 |
| GFAP | 1/200 | Rabbit polyclonal | Dako z 0334 |
| Hoechst 33258 | 1/2000 | | Sigma |

Supplementary Table 7: List of secondary antibodies used for immunostainings.

| Type | Fluorochrome | Dilution | Provider |
|-------------------------|--------------|----------|----------------------|
| Goat anti mouse IgM | AF-555 | 1/500 | Life technologies |
| Rabbit anti mouse IgM | FITC | 1/500 | Life technologies |
| Donkey anti-Goat IgG | AF-555 | 1/500 | Life technologies |
| Donkey anti-Goat IgG | AF-488 | 1/500 | Life technologies |
| Goat anti chicken IgY | AF-488 | 1/500 | Life technologies |
| Goat anti chicken IgY | AF-555 | 1/500 | Life technologies |
| Donkey anti chicken IgY | AF-488 | 1/200 | Jackson laboratories |
| Goat anti mouse IgG | AF-555 | 1/500 | Life technologies |
| Goat anti Rabbit IgG | AF-488 | 1/500 | Life technologies |
| Goat anti Rabbit IgG | AF-555 | 1/500 | Life technologies |
| Donkey anti Rabbit IgG | AF-647 | 1/500 | Life technologies |
| Donkey anti Goat IgG | AF-555 | 1/500 | Life technologies |
| Donkey anti Goat IgG | AF-488 | 1/500 | Life technologies |
| Donkey anti Rabbit IgG | AF-488 | 1/500 | Life technologies |
| Donkey anti Rabbit IgG | AF-555 | 1/500 | Life technologies |
| Donkey anti Rat IgG | AF-488 | 1/500 | Life technologies |
| Donkey anti Chicken IgY | Cy3 | 1/500 | Life technologies |

SUPPLEMENTAL EXPERIMENTAL PROCEDURES

Generation of lentiviral vectors

We selected 16 human transcription factors (TFs) involved in OL differentiation: *ASCL1*, *AXIN2*, *MYRF*, *MYT1*, *OLIG1*, *OLIG2*, *NKX2-2*, *NKX6-1*, *NKX6-2*, *SOX2*, *SOX8*, *SOX9*, *SOX10*, *ST18*, *ZEB2* and *ZNF536* (Cahoy JD *et al.*, 2008, Liu J *et al.*, 2010, Pozniak CD *et al.*, 2010, Weng Q *et al.*, 2012, Najm FJ *et al.*, 2013, Yang N *et al.*, 2013). The coding sequences (CDS) of these genes were PCR amplified (Phusion® High-Fidelity DNA Polymerase, NEB, England) either from total human brain cDNA, from plasmids containing the CDS or from hESC-derived OPCs (generated by previously established protocols) (Douvaras P *et al.*, 2015). The primers contained EcoRI restriction sites (sequence of primers used for the amplification of the TFs are specified on Supp. Table 3) to allow easy integration in the lentiviral vector FUW-OSKM from which the OSKM was excised (a gift from Rudolf Jaenisch, Addgene plasmid # 20328) (Carey BW *et al.*, 2009) (Figure S1). Restriction digestion pattern and DNA sequence analysis were performed to demonstrate the integrity and correct sequence of the cloned TF CDS.

Each TF containing lentiviral vector, as well as the lentiviral plasmid FUW-M2rtTA (Addgene 20342) expressing the reverse tetracycline transactivator (rtTA), were co-transfected with the packaging (psPAX2, Cat No. 12260, Addgene, Cambridge, USA) and the envelope (pMD2. G, Cat No. 12259 Addgene, Cambridge, USA) plasmids into the Lenti-X™ 293T cell line (Cat No. 632180, Clontech, CA, USA) using Fugene transfection reagent (Cat No. E2311, Promega, Madison, WI, USA). Supernatants containing the lentiviral particles were collected after 48hr, filtered through a 0.45µm filter (Millipore) and stored at -80 °C for future use.

The lentiviral reporter system *EF1a-mCherry/MCS5-Sox10-eGFP* was a gift from Prof. Fraser Sim, University of Buffalo, and was produced as the vectors described above. This construct was validated in positive (hESC-derived OPCs, generated as previously described) (Douvaras P *et al.*, 2015) and negative (human fibroblast line BJ1) cell lines (data not shown).

Human ESC/iPSC lines and culture conditions

The following hPSC lines were used in this study: the hESC line H9 (WA09, purchased from WiCell Research Institute), the hiPSC ChiPSC6b line (purchased from Takara Bio Inc.), the hiPSC BJ1 line (generated in our lab (Raitano S *et al.*, 2015) from BJ fibroblasts, ATCC® CRL-2522™), the hiPSC Sigma line (iPSC EPITHELIAL-1 IPSC0028, purchased from Sigma-Aldrich, USA) two iPSC lines derived from primary progressive multiple sclerosis patients (MS-1001-10006-102/-104, purchased from New York Stem Cell Foundation) and two iPSC lines derived from patients with familial forms of amyotrophic lateral sclerosis with the mutations *SOD1-A4V* (purchased from Coriell Institute) and *C9ORF72* (C9 24-4, Guo W *et al.*, 2017). hPSCs were maintained in feeder free conditions using mTESR1 medium (Stemcell Technologies) on hESC-qualified matrigel (Becton Dickinson), splitting twice a week using EDTA (Lonza).

Generation of neural precursor cells (NPCs) and oligodendrocyte lineage cells from hPSCs

hPSCs were dissociated into single cells (accutase, Sigma), seeded at 20.000 cells/cm² on human matrigel-coated plates and cultured in mTESR1 medium containing 1:100 of Rock inhibitor analog (Revitacell, Life Technologies) for 2 days. On day 0, medium was switched to N2B27 medium (DMEM/F12 supplemented with N2 (1:100), B27 (1:50), glutamax (1:100), NEAA (1:100), beta-mercaptoethanol (1:1000), Pen/Strep (1:100), (all from Life Technologies) and 25 µg/ml insulin

(Sigma)), supplemented with the small molecules SB431542 10 μ M (Tocris) and LDN193189 1 μ M (Miltenyi Biotec) and 100nM retinoic acid (RA; Sigma). Medium was changed daily until day 8, at which time SB431542 and LDN193189 were withdrawn and 1 μ M Smoothed agonist (SAG; EMD Millipore) was added to the medium. On day 12, cells were dissociated and plated for further differentiation.

For the initial screen of the 16 TFs, NPCs were expanded for 4-5 passages in N2B27 media with addition of 0.1 μ M RA, 1 μ M SAG and 20 ng/ μ l bFGF (Peprotech). For experiments performed with the 6 selected TFs or *SOX10* alone, NPCs were dissociated on day 12 and immediately subjected to OL lineage differentiation.

For OL lineage differentiation, d12 (or expanded) NPCs were plated at 50.000 cells/cm² on poly-L-ornithine/laminin (Sigma) coated dishes and transduced with each lentiviral vector alone, or combinations of viral vectors, at a multiplicity of infection of 1 or 1.5. The day following transduction, medium was changed to OL differentiation medium (N2B27 supplemented with 10 ng/ml of PDGF α , 10 ng/ml IGF1, 5 ng/ml HGF, 10 ng/ml NT3 (all from Peprotech), 100 ng/ml biotin, 1 μ M cAMP, and 60 ng/ml T3 (all from Sigma)) with the addition of 1 μ g/ml doxycycline (Sigma). Cells were maintained in OL differentiation medium with doxycycline for 7 (initial screen) or 10 days (screen with selected TFs), changing medium every other day.

O4 purification and cryopreservation

Cells maintained for 10 days in OL differentiation media were purified using O4 microbeads (Miltenyi Biotec), used per manufacturer instructions. Purity was checked in all cases by FACS, obtaining >95% O4⁺ purity of the isolated population. Purified O4⁺ cells were used for transcriptome analysis or co-culture with neurons, or cryopreserved till further use. For cryopreservation, the O4⁺ purified fraction was resuspended in OL differentiation medium and mixed 1:1 with ice-cold ProFreeze medium (Lonza) containing 15% DMSO. Cells were immediately stored in a freezing container at -80 °C overnight and transferred the next day to liquid nitrogen for long-term storage. Post-thawing viability was determined by counting the cells with trypan blue in a hemocytometer.

Generation of OLs from hESCs recombined with *SOX10* and *SOX10-GFP* constructs in the *AAVS1* locus

The FRT-cassette containing H9-hESC line described in (Ordovás L *et al.*, 2015) was used to recombine a *SOX10* or *SOX10-GFP* containing plasmid (Figure S4) into the *AAVS1* locus following nucleofection. After positive and negative selection using puromycin and FIAU (Ordovás L *et al.*, 2015), stable cell lines expressing the *SOX10* or *SOX10-GFP* cassettes in an inducible manner were obtained. Doxycycline response experiments were performed to assess the purity and dose response of the cell lines.

Proper cassette integration was tested using junction assay PCRs using 40 ng of genomic DNA with Go Taq DNA polymerase (Promega) in 10 μ l reactions. Primer sequences and PCR program conditions are described in Supp. Table 4. PCR products were loaded on 1.5% agarose (Sigma) gels and visualized with SybrSafe (Invitrogen) on a Gel Doc™ XR+ System (Bio-Rad).

To induce OL differentiation, NPC induction was performed for only 8 days (day 0-5: N2B27 medium containing 10 μ M SB431542, 1 μ M LDN193189 and 100nM RA; day 5-8: same medium with addition of 1 μ M SAG). On day 8, cells were dissociated and seeded at 25.000 cells/cm² on poly-L-ornithine/laminin coated dishes in OL differentiation medium with 2 μ g/ml doxycycline (optimal concentration previously tested) and cultured for up to 17 days.

Myelination assays in shiverer mouse brain slices

Mouse organotypic cortex slices were established according to Stoppini *et al.* (Stoppini L *et al.*, 1991), with modifications. All animal procedures were approved by a Dutch Ethical Committee for animal experiments. Briefly, homozygous shiverer (shi/shi) pups (C3Fe.SWV-Mbpshi, Jackson Laboratory), identified by PCR and confirmed by lack of MBP staining, were sacrificed between postnatal days 3 and 5. The brain was rapidly removed and transferred to ice cold Gey's Balanced Salt Solution (Sigma-Aldrich) containing 5.4 mg/ml glucose and 1% penicillin/streptomycin (P/S, Thermo Fisher Scientific). Fronto-parietal coronal slices (300 μm of thickness) were obtained using a tissue chopper (Mcllwain). Slices were cultured on an air-fluid interface at 37°C with 5% CO₂, using culture plate inserts (0.4 μm pore size, 30 mm diameter, Millipore) in 50% MEM α , 25% HBSS, 25% horse serum, 6.5 mg/mL glucose, 2 mM glutamine, 1% N2 supplement and 1% P/S (all Thermo Fisher Scientific), supplemented with 100ng/ml biotin, 60ng/ml T3, 25 $\mu\text{g}/\text{ml}$ insulin, 20 $\mu\text{g}/\text{ml}$ ascorbic acid, 1 $\mu\text{g}/\text{ml}$ of doxycycline (all Sigma-Aldrich) and 1 μM cAMP (Thermo Fisher Scientific). Three days after slicing, slices of homozygous shi/shi were transplanted with 1×10^4 purified O4⁺ cells in 1.0 μL PBS using a Picospritzer. O4⁺ cells were allowed to mature into myelinating OLs for 10 days after injection, in the absence of doxycycline for the last 5 days of culture, when the slices were fixed (4% formalin in PBS) and stained for primary and secondary antibodies (diluted in 0.05 M Tris, 0.9% NaCl, 0.25% gelatin and 0.5% Triton-X-100 (pH 7.4)). Samples were imbedded in Mowiol 4-88 (Fluka) after which confocal imaging was performed with a Zeiss LSM700 confocal microscope using ZEN software (Zeiss).

Co-culture with neurons

Cortical neurons were generated from WT hPSCs based on previously described methods (Shi Y *et al.*, 2012). Neuronal progenitors obtained after 3 neuronal rosette isolations steps and 4 cell passages (~50 days) were seeded at 50.000 cells/ cm^2 on poly-L-ornithine/laminin coated dishes and allowed to mature for 10-14 days in Neural Maintenance Medium (NMM, 1:1 mix of DMEM/F12 and neurobasal media, supplemented with N2 (1:200), B27 (1:100), glutamax (1:100), NEAA (1:200), beta-mercaptoethanol (1:2000), Pen/Strep (1:200), L-glutamine (1mM) (all from Life Technologies) and 2.5 $\mu\text{g}/\text{ml}$ of insulin (Sigma).

O4⁺ cells were purified by immunomagnetic beads from day 8-10 *SOX10*-transduced progeny and seeded at 50.000 cells/ cm^2 on the maturing neurons. Cultures were maintained for 20 days in co-culture media (NMM supplemented with 100 ng/ml of biotin, 1 μM of cAMP, insulin (25 $\mu\text{g}/\text{ml}$), T3 (60 ng/ml), ascorbic acid (AA, 20 $\mu\text{g}/\text{ml}$, Sigma) and 1 $\mu\text{g}/\text{ml}$ doxycycline (Sigma)) with partial medium replacement every 2-3 days. Doxycycline was removed from day 10 onwards to assess OL maturation in the absence of *SOX10* overexpression.

Adaptation of co-culture for high-throughput screening:

To adapt the O4⁺ cell-neuron culture system to 96 and 384 well plate format, purified O4⁺ cells were seeded at 50.000 cells/ cm^2 on neurons generated by culture of cortical NPCs at 50.000 cells/ cm^2 and allowed to mature for 2 weeks. O4⁺ cells were allowed to attach for 2-3 h before addition of the different compounds to the co-culture medium (as described above for co-culture media but without T3 and AA) in the presence of doxycycline. Cell culture conditions used were: control (0.1% DMSO), +T3 (60 ng/ml), +DAPT (N-[(3,5-Difluorophenyl)acetyl]-L-alanyl-2-phenyl]glycine-1,1-dimethylethyl ester, 1 μM , Tocris), +Pranlukast (22.8 μM , Selleckchem), +Clobetasol propionate (5 μM , Selleckchem)

and +Miconazole (1 μ M, Selleckchem). Media with corresponding compounds were exchanged twice a week.

Based on MBP expression, three variables were assessed: total MBP⁺ area, number of MBP⁺ cells and total intensity of the identified MBP⁺ area (MBP⁺ Intensity). Differences in the MBP⁺ area between control and different compounds/drugs in the co-culture system were tested using matched-pairs t-tests using JMP pro12 from SAS institute (www.sas.com) (Supplementary Figure 5). Variables with p-values less than 0.05 were considered statistically significant.

Flow cytometry and cell sorting

Cells were enzymatically harvested using accutase, centrifuged and resuspended in 100 μ l FACS buffer (PBS 1x, 2% fetal bovine serum and 0.02% sodium azide).

To determine O4 expression, cells were incubated with 1/20 dilution of the O4-APC antibody or isotype control (Miltenyi Biotec) for 15 min at 4 °C, washed and resuspended in 150 μ l FACS buffer. Cells were analyzed on a FACS Canto flow cytometer using the FACS DIVA software (Becton & Dickinson). After exclusion of cell doublets, gates were established based on the corresponding isotype controls.

To analyze the expression of the mCherry/MCS5-SOX10-eGFP reporter, cells were analyzed on a FACS Aria III (equipped with the 561nm laser) using the FACS DIVA software (Becton & Dickinson). Thresholds were set based on untransduced cells.

O4⁺ cells and O4⁻ cells were FACS selected from day 10 *SOX10*-transduced progeny on a FACS Aria III using the FACS DIVA software. To isolate O4⁺ cells for subsequent cultures, immunomagnetic separation using anti-O4 Microbeads (Miltenyi Biotec) was performed following the manufacturer's recommendations. Purity was checked afterwards by FACS, yielding always >95% of O4⁺ cells in the purified population.

All results were analyzed using Flow Jo (FlowJo, LLC, USA) and FACS DIVA software (Becton & Dickinson). Flow cytometry and FACS sorting was performed at the KU Leuven Flow Cytometry Facility.

RNA extraction, cDNA synthesis and gene expression

Total RNA was purified using the GenElute™ Mammalian Total RNA Miniprep Kit (Sigma-Aldrich, Saint Louis, MO, USA) and ZR RNA MicroPrep (Zymo Research, CA, USA). After concentration and integrity validation (NanoDrop 1000, Thermo Fisher Scientific, MA USA), cDNA was generated using 0.5-1 μ g of RNA with SuperScript® III First-Strand Synthesis SuperMix for qRT-PCR kit (Invitrogen, CA, USA) and qRT-PCR was performed in technical triplicates on a ViiA™ 7 Real-Time PCR System with 384-well plate (Applied Biosystems, Carlsbad, CA, USA) with a Platinum® SYBR® Green qPCR SuperMix-UDG w/ROX (Invitrogen, CA, USA) and primers mix at final concentration of 250 nM.

Gene expression (Cycle threshold) values were normalized based on the *GAPDH* (Glyceraldehyde 3-phosphate dehydrogenase) housekeeping gene and the Delta CT calculated. Gene specific primers were designed in exon-exon spanning regions in common domains of all isoforms described for a given gene. To distinguish endogenous from transgene expression, primers were designed covering the 3' untranslated regions and were named as the name of the gene followed by *e* (*ASCL1e*, *OLIG2e*, *SOX2e* and *SOX10e*). The efficiency of primers was tested by serial dilutions of cDNA and by calculating the coefficient of regression (R^2). An efficiency of 90-105% with an $R^2 \geq 95\%$ was accepted (see Supp. Table 5 for a list of all qRT-PCR primers used in this study).

Transcriptome analysis by RNA sequencing

Total RNA was purified using the GenElute™ Mammalian Total RNA Miniprep Kit (Sigma). RNA concentration and purity were determined spectrophotometrically using the Nanodrop ND-1000 (Nanodrop Technologies) and RNA integrity was assessed using a Bioanalyzer 2100 (Agilent). Per sample, an amount of 100 ng of total RNA was used as input. Using the Illumina TruSeq® Stranded mRNA Sample Prep Kit (protocol 15031047 Rev.E "October 2013") poly-A containing mRNA molecules were purified from the total RNA input using poly-T oligo-attached magnetic beads. In a reverse transcription reaction using random primers, RNA was converted into first strand cDNA and subsequently converted into double-stranded cDNA in a second strand cDNA synthesis reaction using DNA Polymerase I and RNase H. The cDNA fragments were extended with a single 'A' base to the 3' ends of the blunt-ended cDNA fragments after which multiple indexing adapters were ligated, introducing different barcodes for each sample. Finally, enrichment PCR was carried out to enrich DNA fragments that had adapter molecules on both ends and to amplify the DNA in the library. Sequence-libraries of each sample were equimolar pooled and sequenced on an Illumina NextSeq 500 instrument (High Output, 75 bp, Single Reads, v2) at the VIB Nucleomics core (www.nucleomics.be).

Low quality ends and adapter sequences were trimmed off from the Illumina reads. Subsequently small reads (length < 35 bp), ambiguous reads (containing N) and low quality reads (more than 50% of the bases < Q25) were filtered. Processed reads were aligned with Tophat v2.0.8b to the Human reference genome (GRCh38), as downloaded from the Genome Reference Consortium (<https://www.ncbi.nlm.nih.gov/grc/human/data>). Default Tophat parameter settings were used, except for 'min-intron-length=50', 'max-intron-length=500,000', 'nocoverage-search' and 'read-realign-edit-dist=3'.

Transcriptome datasets used in the comparison were downloaded from Gene Expression Omnibus (GEO). Raw values of different brain cell types from the cortex were obtained from GSE73721 (Zhang Y *et al.*, 2016). We also downloaded microarray data of different stages of oligodendrocyte maturation from GSE32589 (Abiraman K *et al.*, 2015).

RNA-seq data were aligned using Tophat2 and RPKM values were computed using Cufflink. All RNA-seq data was then normalized using upper quartile normalization. Each sample in the microarray dataset was normalized using linear normalization with a mean intensity of 500. Data across the different publication datasets were then combined with our RNA-seq data based on matching ENSEMBL identifiers. Hierarchical clustering showed that data from each batch would cluster according to the study, therefore an empirical Bayes method (Johnson WE *et al.*, 2007) was used to eliminate the batch effects to allow for data comparison. The batch correction was carried out in the statistical software, R treating each individual study as a batch. Principal component analysis and hierarchical clustering were performed using the OmicsOffice package built in TIBCO Spotfire v7.6. Different samples in TIBCO Spotfire were clustered by complete linkage method and their similarity was measured as city-block distance for hierarchical clustering. Visualization of the gene expression was also carried out using TIBCO Spotfire.

Differentially expressed genes were identified using the 'Samr' package in the statistical software, R. The threshold criteria of FDR > 0.05 and a fold change of two or more in gene expression among the different pair-wise comparison was used to identify the differentially expressed genes. Gene ontology

(GO) of the different differentially expressed genes were carried out using the Gene Ontology Consortium (<http://www.geneontology.org/>).

Immunostainings

Cells were washed with PBS 1x and fixed for 15 min at RT with 4% formaldehyde solution and washed with PBS. Preparations were permeabilized in 0.1% Triton-X-100 (Sigma) (step omitted for O4 and O1 antigens) and blocked in 10% donkey or goat serum (Dako) in PBS for 1h at RT. Primary antibodies were incubated overnight at 4 °C in 5% in donkey or goat serum in PBS, washed 3 times, and incubated for 1h at RT with fluorescently-labeled secondary antibodies diluted to 1:500. Samples were incubated for 15 min at RT with Hoechst 33258 (1:2000 dilution) for nuclear staining and mounted with ProLong[®] Gold Antifade Mountant (Thermo Fisher Scientific). The list of primary and secondary antibodies and the dilutions used can be found in Supp. Tables 6 and 7.

Image acquisition and analysis

The immunostained cells were examined using an Axioimager.Z1 microscope (Carl Zeiss). For quantification purposes, at least 5 independent fields per condition and per experiment were obtained. Confocal images of the neuron-OL co-cultures were obtained using a C LSM 510 Meta NLO confocal microscope (Carl Zeiss). For the initial screen using the A2B5 marker as well as for the evaluation of the miniaturized co-culture system, images were acquired on an InCell Analyzer 2000 High Content Imager (GE Healthcare), acquiring sufficient numbers of images to cover at least 70% of the well area. For A2B5, quantification was performed using the InCell image analysis software (GE Healthcare). For the co-cultures, batch analysis were performed using a developed script on ImageJ software, where MBP expression and regions of interest were elucidated based on intensity threshold and presence of staining debris were removed from the selection based on size and circularity parameters.

Preparation of transmission electron microscopy samples.

Cells were seeded on Thermanox[®] slides and fixed with 2% glutaraldehyde in 0.05M sodium cacodylate buffer. Following fixation, cells were postfixed in 2% osmium tetroxide for 1 hour and stained with 2% uranyl acetate in 10% acetone for 20 min. Subsequently, the cell-seeded coverslips were put through a dehydrating series of graded concentrations of acetone and embedded in araldite or durcupan resin (Sigma) according to the pop-off method (Bretschneider A *et al.*, 1981). Semi-thin sections (0.5-1 μ m) were performed and stained with toluidine blue for the identification of regions of interest. Ultra-thin sections (60-80 nm) were mounted on 0.7% formvar-coated grids, contrasted with uranyl acetate and lead citrate, and examined with a Philips EM 208 transmission electron microscope or JEOL JEM1400 electron microscope operated at 80 kV. Digital images were captured using a Morada camera system. For quantification purposes, images were analyzed using SIS analysis software (Germany).

Statistical analysis

Comparisons between two groups were analyzed using unpaired or paired 2-tailed Student's t test. P-values < 0.05, were considered significant (*). Data are shown as mean and error bars represent standard error of mean (SEM) of a minimum three independent experiments. Results were plotted and analyzed using GraphPad Prism 6 software.

REFERENCES

- Abiraman K, Pol SU, O'Bara MA, Chen GD, Khaku ZM, Wang J, Thorn D, Vedia BH, Ekwegbalu EC, Li JX, Salvi RJ, Sim FJ. Anti-muscarinic adjunct therapy accelerates functional human oligodendrocyte repair. *J Neurosci*. 2015 Feb 25;35(8):3676-88.
- Bretschneider A, Burns W, Morrison A. "Pop-off" technic. The ultrastructure of paraffin-embedded sections. *Am J Clin Pathol*. 1981;76(4):450-3.
- Cahoy JD, Emery B, Kaushal A, Foo LC, Zamanian JL, Christopherson KS, Xing Y, Lubischer JL, Krieg PA, Krupenko SA, Thompson WJ, Barres BA. A transcriptome database for astrocytes, neurons, and oligodendrocytes: a new resource for understanding brain development and function (2008). *J Neurosci*. 2008 Jan 2;28(1):264-78.
- Carey BW, Markoulaki S, Hanna J, Saha K, Gao Q, Mitalipova M, Jaenisch R. Reprogramming of murine and human somatic cells using a single polycistronic vector (2009). *Proc Natl Acad Sci U S A*. 2009 Jan 6;106(1):157-62.
- Douvaras P, Fossati V. Generation and isolation of oligodendrocyte progenitor cells from human pluripotent stem cells. *Nat Protoc*. 2015 Aug;10(8):1143-54.
- Guo W, Naujock M, Fumagalli L, Vandoorne T, Baatsen P, Boon R, Ordovás L, Patel A, Welters M, Vanwelden T, Geens N, Tricot T, Benoy V, Steyaert J, Lefebvre-Omar C, Boesmans W, Jarpe M, Sternecker J, Wegner F, Petri S, Bohl D, Vanden Berghe P, Robberecht W, Van Damme P, Verfaillie C, Van Den Bosch L. HDAC6 inhibition reverses axonal transport defects in motor neurons derived from FUS-ALS patients. *Nat Commun*. 2017 Oct 11;8(1):861.
- Johnson WE, Li C, Rabinovic A. Adjusting batch effects in microarray expression data using empirical Bayes methods. *Biostatistics*. 2007 Jan;8(1):118-27.
- Liu J, Sandoval J, Doh ST, Cai L, López-Rodas G, Casaccia P. Epigenetic modifiers are necessary but not sufficient for reprogramming non-myelinating cells into myelin gene-expressing cells (2010). *PLoS One*. 2010 Sep 27;5(9):e13023.
- Najm FJ, Lager AM, Zaremba A, Wyatt K, Caprariello AV, Factor DC, Karl RT, Maeda T, Miller RH, Tesar PJ. Transcription factor-mediated reprogramming of fibroblasts to expandable, myelinogenic oligodendrocyte progenitor cells (2013). *Nat Biotechnol*. 2013 May;31(5):426-33.
- Ordovás L, Boon R, Pistoni M, Chen Y, Wolfs E, Guo W, Sambathkumar R, Bobis-Wozowicz S, Helsen N, Vanhove J, *et al*. Efficient Recombinase-Mediated Cassette Exchange in hPSCs to Study the Hepatocyte Lineage Reveals AAVS1 Locus-Mediated Transgene Inhibition. *Stem Cell Reports*. 2015 Nov 10;5(5):918-31.
- Pozniak CD, Langseth AJ, Dijkgraaf GJ, Choe Y, Werb Z, Pleasure SJ. Sox10 directs neural stem cells toward the oligodendrocyte lineage by decreasing Suppressor of Fused expression (2010). *Proc Natl Acad Sci U S A*. 2010 Dec 14;107(50):21795-800.
- Raitano S, Ordovás L, De Muyenck L, Guo W, Espuny-Camacho I, Geraerts M, Khurana S, Vanuytsel K, Tóth BI, Voets T, Vandenberghe R, Cathomen T, Van Den Bosch L, Vanderhaeghen P, Van Damme P, Verfaillie CM. Restoration of progranulin expression rescues cortical neuron generation in an induced pluripotent stem cell model of frontotemporal dementia. *Stem Cell Reports*. 2015 Jan 13;4(1):16-24.
- Shi Y, Kirwan P, Smith J, Robinson HP, Livesey FJ. Human cerebral cortex development from pluripotent stem cells to functional excitatory synapses. *Nat Neurosci*. 2012 Feb 5;15(3):477-86, S1.
- Stoppini L, Buchs P, A. & Muller, D. A simple method for organotypic cultures of nervous tissue. *J. Neurosci. Methods* 37, 173–82 (1991).

Weng Q, Chen Y, Wang H, Xu X, Yang B, He Q, Shou W, Chen Y, Higashi Y, van den Berghe V, *et al.* Dual-mode modulation of Smad signaling by Smad-interacting protein Sip1 is required for myelination in the central nervous system (2012). *Neuron*. 2012 Feb 23;73(4):713-28.

Yang N, Zuchero JB, Ahlenius H, Marro S, Ng YH, Vierbuchen T, Hawkins JS, Geissler R, Barres BA, Wernig M. Generation of oligodendroglial cells by direct lineage conversion (2013). *Nat Biotechnol*. 2013 May;31(5):434-9.

Zhang Y, Sloan SA, Clarke LE, Caneda C, Plaza CA, Blumenthal PD, Vogel H, Steinberg GK, Edwards MS, Li G, *et al.* Purification and Characterization of Progenitor and Mature Human Astrocytes Reveals Transcriptional and Functional Differences with Mouse. *Neuron*. 2016 Jan 6;89(1):37-53.